NASW-4435

DESIGN OF EQUIPMENT FOR LUNAR DUST REMOVAL

Submitted to:
Dr. Kristin Wood

For:
M.E. 397
Advanced Engineering Design:
Theory, Techniques, and Automation
And
The NASA/USRA University
Advanced Design Program

Prepared by:
Lacy Belden
Kevin Cowan
Hank Kleespies
Ryan Ratliff
Oniell Shah
Kevin Shelburne

Mechanical Engineering Department
THE UNIVERSITY OF TEXAS AT AUSTIN
Austin, Texas

Spring 1991

ABSTRACT

NASA has a long range goal of constructing a fully equipped, manned lunar base on the near side of the moon by the year 2015. During the Apollo missions, lunar dust coated and fouled equipment surfaces and mechanisms exposed to the lunar environment. In addition, the atmosphere and internal surfaces of the lunar excursion module were contaminated by lunar dust which was brought in on articles passed through the airlock. Consequently, the need exists for a device or appliance to remove lunar dust from equipment and finished surfaces. Five concepts were investigated to determine their effectiveness in removing lunar dust from surfaces of material objects used outside of the proposed lunar habitat. Additionally, several concepts were investigated for preventing the accumulation of lunar dust on mechanisms and finished surfaces.

The character of the dust and the lunar environment present unique challenges for the removal of contamination from exposed surfaces. In addition to a study of lunar dust adhesion properties, the project examines the use of various energy domains for removing the dust from exposed surfaces. Also, prevention alternatives are examined for systems exposed to lunar dust.

A concept utilizing a pressurized gas is presented for dust removal outside of an atmospherically controlled environment. The concept consists of a small astronaut/robotic compatible device which removes dust from contaminated surfaces by a small burst of gas.

TABLE OF CONTENTS

LIST OF FIGURES

1.0 INTRODUCTION

The National Aeronautics and Space Administration conducted several exploratory missions to the moon during the period from 1969 through 1973. These missions, known as the Apollo program, resulted in the accumulation of an enormous amount of data pertaining to the composition and geology of Earth's only natural satellite. During the course of these information gathering missions, the astronauts observed that the layer of dust covering the surface of the moon exhibited a high affinity for material objects. Items such as the space suits, hand tools, optical equipment and mechanical equipment with moving parts were representative of the objects the lunar dust adhered to quite readily. This layer of material, known as the lunar regolith, produced numerous unforeseen problems during the Apollo missions. Most notably, the dust impaired the proper operation of seals and lubricants used on various mechanisms and also accumulated heavily on exposed optical surfaces. In addition, the atmosphere and internal surfaces of the lunar excursion module were contaminated by lunar dust which was brought in on articles passed through the airlock.

It is anticipated that the United States will begin construction of a lunar base by the turn of the century. Establishment and operation of this base will result in repeated and continual exposure of equipment and space suits to the lunar surface. As a result of the large scale dust contamination which is anticipated during construction and operation of the base, an urgent need exists for a device or system which will effectively clean lunar dust from material surfaces without altering the quality of the surface finish.

The objective of this project was to design a system or a device which will effectively remove lunar dust from material surfaces in a zero atmosphere, one-sixth gravity environment. Due to the number of different materials and surface geometries encountered in this project, it was necessary to narrow the scope of the task to make it more tractable for a one semester design problem. The scope of the project was restricted to the design of a device which is capable of removing lunar dust from delicate optical surfaces such as camera lenses and mirrors. This particular material surface was selected for study because of its inherent delicate nature. A

design capable of successfully removing lunar dust from optical surfaces without altering the operational capabilities of these devices may be extended to cleaning other devices where surface finish is not of great importance. This would include space suits, painted surfaces, and mechanical equipment with various moving parts.

This report sets forth the general project requirements, the environmental constraints which the conceptual design must satisfy to achieve the intended function, a description of alternative designs using various energy domains, and provides a detailed description of the final design solution. The conclusions and recommendations section provides information for extending this work beyond the current scope of the project.

1.1 Project Requirements

Three main requirements governed this project:

1. Characterize the use of various energy domains for achieving the aforementioned goals in a one-sixth gravity, zero atmosphere environment.

2. Design a device or system which will be capable of removing lunar dust from optical surfaces without altering the surface finish.

3. Propose methods of preventing lunar dust from accumulating on finished surfaces.

1.2 Design Specifications

A detailed list of the design specifications for this project is given in Appendix 1. The following section on the lunar environment details some of the important aspects pertaining to this project.

1.3 Lunar Environment

The lunar environment will present unique circumstances and constraints that the final design solution must satisfy to achieve its intended function. The primary objective of the project is to design a device for removing lunar dust from optical surfaces in the harsh lunar environment. Therefore, it will be necessary to ascertain the characteristics with which the device must contend. The following information provides a description of the lunar environmental aspects which must be considered for designing dust removal equipment.

1.3.1 Temperature

The temperature on the lunar surface varies over a wide range of values. Daytime temperatures, which occur when the sun's rays are directly incident on the lunar surface, approach 384 K (232 °F) in the equatorial regions of the moon. Lunar night temperatures are as low as 102 K (-276 °F). Temperature extremes on the order of 44 K (- 380° F) are possible in the permanently shadowed areas near the lunar poles [41].

Problems commonly associated with high temperatures of the lunar day include severe outgassing of materials and lubricants and large strains due to thermal gradients which exist between sunlit and shaded sides of equipment [41]. Outgassing occurs when the temperature of a material object is high enough to produce evaporation of some of the molecules. This promotes rapid degradation of the material characteristics. Any equipment reliant on lubrication and seals must be carefully designed so that the lubricant does not evaporate and increase the frictional characteristics and hence the power requirements of the device. Also, as mentioned previously, thermal gradients arise from the differential heating between the sunlit and shaded sides of exposed surfaces. Materials which possess a low coefficient of thermal expansion should be considered for this situation in order to minimize thermal strains.

Low temperatures produce embrittlement of certain materials [41]. This will result in component failure at a smaller value of stress than normally anticipated because of the reduction in ductility. This condition

must be accounted for when selecting materials for fabrication of the device. Materials which exhibit favorable characteristics in a cryogenic (extremely low temperature) environment will be suitable for such applications.

1.3.2 Vacuum

Since the moon is absent of any significant atmosphere, pressure generally ranges from 10^{-6} to 10^{-10} Pascals, which is a near perfect vacuum [41]. The main problems associated with the lunar vacuum are similar to those previously mentioned with high temperatures, namely outgassing. Outgassing occurs because of either extremely high temperatures or very low pressures. Vacuum conditions destroy surface films which are normally present on physical objects in a terrestrial environment [41]. Surface films on material objects are due to gases, vapors and oxides present in the Earth's atmosphere. Since the moon is void of an atmosphere these surface films do not exist. This increases surface friction between moving parts. As a result, equipment design must account for the possibility of outgassing and should therefore require a minimum number of components susceptible to this type of degradation.

1.3.3 Gravity

Gravity varies in magnitude over the entire surface of the moon. By and large, the acceleration due to gravity on the moon is taken to be one-sixth the value experienced on Earth [46]. Although physical objects will weigh less on the surface of the moon, care must be taken to minimize the mass of equipment because inertial effects remain the same as on Earth.

1.3.4 Micrometeorites

Micrometeorites are high velocity, low mass, microscopic cosmic particles which collide with material objects present in the lunar environment. Particle mass ranges in value from 10^{-7} to 10^{-4} grams and have an average speed of 20,000 meters per second [41]. These high velocity impacts will produce pitting of exposed surfaces which could lead

to premature equipment failure. While micrometeorite impact is not as frequent as it once was, destruction of exposed surfaces is still possible. Information obtained from the Surveyor 3 experimental spacecraft indicates that the micrometeorite flux received on the moon may be great enough to impair operation of optical equipment [14]. Design of equipment to be used outside of the lunar habitat should include protection as a precaution against micrometeorite impact.

1.3.5 Lunar Regolith

The surface of the moon is covered with a layer of meteorite generated debris known as lunar regolith. The regolith consists of a mixture of poorly sorted fragmental debris that ranges in size from very small particles to large rocks 0.8 meters in diameter. Surface regolith is porous and weakly coherent. It is relatively easy to trench to depths of several centimeters and is easily disturbed by kicking or walking [41].

Dust on the lunar surface behaves differently than terrestrial dust because of the lack of an atmosphere. Dust is not stirred up and carried by wind currents as on Earth and as a result remains stable unless dislodged by kicking or micrometeorite impact. If lunar dust is dislodged from the surface of the moon, the particles will remain spaceborne for a longer period of time [41]. This is due to the lack of an atmosphere and to the reduced lunar gravitational attraction. Consequently, the dust travels longer distances and has more opportunity to make contact with material surfaces . Therefore, the device should be designed so that it is not susceptible to contamination also.

1.3.6 Summary

The lunar environment presents many challenges and obstacles which must be addressed in designing equipment for lunar dust removal. Device configuration, sealing mechanisms, and material selection are all of great importance to the durability and effectiveness of the equipment. Attention to detail must not be sacrificed for the sake of simplicity in the final analysis. A feasible working solution which satisfies the aforementioned constraints is presented later in this report.

2.0 LUNAR DUST CHARACTERISTICS

The characterization of the lunar dust is the first step in the search for the solution to the dust adhesion problem. The energy required to break the adhesive bond of the dust to various surfaces is dependent on the dust properties as well as those of the surfaces to which the dust adheres. This section of the report will characterize lunar dust in terms of composition, morphology, and electrostatic charge. In addition, some empirically derived estimates of dust adhesion forces will be discussed. Much of this information is from the results of the "Analysis of Surveyor 3 material and photographs returned by Apollo 12". [15., 38., 44., 49.]

The composition of the lunar dust has been determined through electron microprobe analyses of samples obtained by mean of a cellulose stripping technique. Robertson et. al. [44., pp. 29+] report on the results obtained through analysis of samples taken from the surface of Surveyor 3's clear television camera filter, while Carr and Proudfoot [15., pp. 46+] report on those from the surface of a Surveyor 3 mirror. The results of the studies of Robertson et. al. and Carr and Proudfoot indicate the following average composition of the lunar dust:

SiO_2	39.0 %
FeO	15.8
CaO	17.3
Al_2O_3	19.8
TiO_2	2.6
MgO	3.2
K_2O	0.7
Cr_2O_3	0.06
S	0.3
ZnO_2	0.07

The silicon, ferrous, calcium, and aluminum oxides make up over 90% of the average composition, silicon being the prevalent element. The glassy

composition of the dust accounts for its highly abrasive character. Since the ferrous content is only a small percentage of the overall average composition, the magnetism of the dust is insignificant. Robertson et. al. report that these results for average composition are consistant with previously examined lunar fines and soils. The microprobe data of Robertson et. al. also showed variation among individual dust particle compositions indicating that the particles are mixtures of more than one mineral. [44., p. 45]

The morphology of lunar dust particles was studied with X-ray diffraction by Robertson et. al. and with electron microscopy by Carr and Proudfoot. In general, the shapes of dust particles have been described as 'uniquely shaped', 'fine grain angular fragments', 'spherical', and 'rodlike with bulbous ends'. [38., p. 9, A., p. 34] Scanning electron microscope microphotographs (from Robertson et. al.) in Figure 2.0-1. illustrate some of the typical irregular shapes. In addition, the X-ray examination of individual particles, performed by Robertson et. al., indicates that "... the majority of the particulates are complex mixtures of more than one crystalline phase and not merely micrometer-sized pieces of single-phase materials." [44., p. 45] They conclude that the most likely source of the dust is the lunar breccia. A breccia is a coarse-grained, clastic rock, composed of angular broken rock fragments held together by a mineral cement or a fine-grained matrix; lunar breccias are, in part, the result of crushing and grinding associated with meteorite impact. [2.,56.]

The overall range of particle sizes is approximately 0.2 microns to 40 microns. The size range for dust samples taken from the Surveyor 3 television filter were spread over a range of 2 to 40 microns, with about 90% of the visible material at less than 10 microns. 90% of the size range for the samples taken from the Surveyor 3 mirror are in the range of 0.3 to 3 microns, with 'very few' particles greater than 4 microns. Carr and Proudfoot report that spherical particles from the mirror, as opposed to the fine grained angular fragments, tended toward a smaller size range, with the majority at 0.2 micron diameter. [15., p. 47+] The surface finish for optical surfaces is on the order of the size of the smallest particles at 0.1 to 0.2 microns. It is these smaller particles that will adhere more

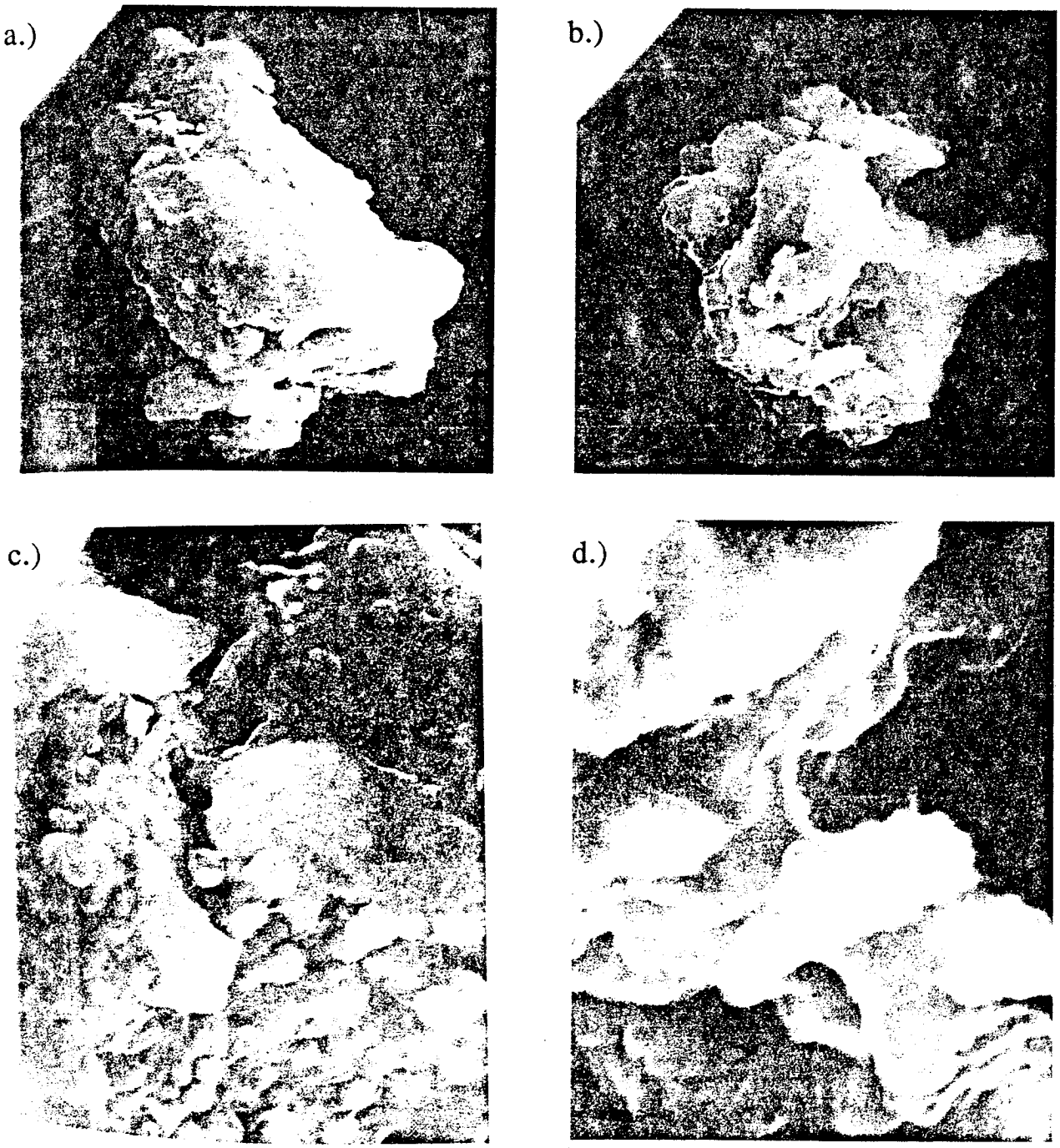

Figure 2.0-1: Scanning electron microscope photomicrographs of typical dust particles. a.) 2,000 X, b.) 4,000 X, c.) 15,000 X, d.) 15,000 X
from *Robertson, et. al. "Characterization of dust on clear filter from returned Surveyor 3 television camera"* [44.]

strongly because of a greater contact area to particle mass ratio. The 'smooth' surface of the spherical particles may also allow for more contact area per particle between the particle and the surface to which it adheres. In fact, Scott and Zuckerman, in their analysis of the Surveyor 3's soil sampler scoop, found that the spherical particles adhered more strongly than the jagged, angular fragments (removal with a vacuum from painted surface). [49., p. 114]

Electrostatic charging of the lunar dust is accomplished by the solar wind. [56.] The emission of photoelectrons from the surface of the moon, due to solar radiation, produces electric fields which levitate the charged dust particles 2cm above the lunar surface. The electrostatic lifting of these particles is aided by their 'high' resistivity and extreme retention time of charge. [27.,p.546] The 1/6 g environment and the large surface to volume ratio of the particles insure that the electrostatic surface forces will dominate body forces. The vacuum environment of the moon results in a lack of surface films (gases, vapors, and oxides) which coat soil particles on Earth. The strong adherance of the dust to surfaces is due to the lack of these films that normally act to lower surface energy. [41., pp. 6,20,25]

As determined from the analysis of the Surveyor 3 surface soil sampler scoop, the order of magnitude of dust adhesion is dependent upon the surface to which it adheres. Scott and Zuckerman estimate that the adhesive strength of dust particles to a painted surface is on the order of 689.4 Pa (0.1 psi), while their adhesive strength to metallic surfaces is in the range of 68.94 to 689.4 Pa (0.01 - 0.1 psi). [49., p. 114] In the "Summary and conclusions" section of the Analysis of Surveyor 3 material and photographs returned by Apollo 12, Nickle and Carroll report the adherence strength of dust to Teflon surfaces is between that of painted surfaces and metal surfaces. [38., p.10] Therefore, it is assumed that, as the surface finish becomes smoother, the adhesive strength between the dust and the surface decreases. This implies that the adhesive strength of dust on polished optical surfaces is smaller than that on the aforementioned surfaces.

3.0 ALTERNATIVE DESIGNS

3.1 Prevention

All support equipment for moon base which has the possibility of being exposed to the lunar environment, directly or indirectly, must consider the existence of the lunar dust in its design. Although removal may not be required in some cases, the cleaning task will play a major role in the allocation of crew time and equipment maintenance if prevention measures are not taken. In addition, many items are difficult to clean due to their geometry, scale, surface properties, operating condition, and location. Also, the safety of the crew should not be dependent on regular performance of lunar dust removal from equipment and surfaces.

3.1.2 Prevention Alternatives

Prevention alternatives exist in both hardware and operation design for all systems exposed to the lunar dust. Areas of particular interest are:

- Large surface areas (solar arrays, thermal radiators)
- Optical Equipment (windows, lenses, mirrors)
- Extravehicular Mobility Unit (spacesuit, portable life support)
- Mechanical Systems (lunar rovers, robotics)
- Interfaces (tools, connectors)

These areas were grouped according to the mode in which lunar dust contamination presents the greatest difficulty to their operation. In the following discussion, concepts are presented for the prevention of problems associated with exposure to the lunar dust environment.

3.1.2.1 Large Surface Areas

Large areas such as solar arrays and thermal radiators present a large and possibly critical problem for lunar dust removal [22 pg. 74]. For these surfaces the layer of dust present on the surface will decrease the system's efficiency approximately linearly with the amount of

contamination present [6 pg. 91-96]. All such large surface areas should be designed with a polished outer surface to minimize the adhesion of the dust to the surface and help prevent excessive accumulation. In addition, a polished surface will greatly aid the cleaning task should it be necessary. Since complete removal or prevention of dust on these large exposed surfaces is not possible, all thermal radiators and solar arrays must be designed and sized to account for the loss of efficiency due to the lunar dust layer. This will add another predicted efficiency loss in addition to the loss of efficiency accounted for due to radiation damage [34 pg. 301-305]. In addition, due to the high mobility of the dust and ease at which it becomes spaceborne, operations in the vicinity of solar arrays and thermal radiators should be planned in order to provide the least amount of dust exposure to these mission critical systems.

3.1.2.2 Optical Surfaces

Surfaces such as mirrors, windows, and lenses pose a unique problem for lunar dust removal due to the delicate surface finish which must be preserved. As previously discussed in section 2.0, the hardness and sharpness of the lunar dust crystals prevents direct mechanical removal of the dust particles from optical surfaces. Although dust adhesion to highly polished surfaces is low relative to other exposed surfaces, repeated cleaning and direct contact between the dust and surface should be avoided to prevent damage. As a result, a prevention method should reduce the possibility of dust particles coming in contact with the polished lens surface.

During Apollo 12, astronauts inspected the Surveyor III which was in close proximity to the Apollo 12 landing site. As previously mentioned, a mirror of the Surveyor was completely obscured by the lunar dust disturbed by the landing of the Apollo spacecraft. In general, the primary source of lunar dust mobility is disturbances due to man-systems activities. Therefore, a major role of dust accumulation prevention is to protect optical surfaces from the sources of lunar dust disturbances.

For optical systems which do not require continuous coverage of critical operations, an automated iris may be used. The iris would be closed at times when the view provided is not needed, particularly at times when a local disturbance is generating moving dust [13 pg. 278-287]. In

essence, the iris serves as an automated lens cap. This has the disadvantage of creating another possible failure mode for the camera. Another possibility would be to use orientations of the optical surface which avoid the possibility of the dust settling directly onto the surface. Specifically, orientations which face away from the gravity vector of settling lunar dust.

For optical systems which must provide a continuous view of operations, sacrificial surfaces may be used to mask the critical optical surface. Sacrificial surfaces would consist of thin clear layers of material placed directly over an optical surface. Once an outer layer became sufficiently coated with contamination, it would be removed to reveal a new sacrificial surface layer. Suggestions for the use of sacrificial surfaces can be found in volume 11 of the Man-Systems Integration Standards [33 pg. 48-55]. Some disadvantages of sacrificial surfaces are the probable reduction in optical quality, disposal of the spent protection surfaces, and crew time required to conduct regular maintenance.

3.1.2.3 Extravehicular Mobility Unit (EMU)

The EMU consists of the spacesuit, portable life support system, and any associated support equipment. Primarily, the cleaning difficulty of the EMU is determined by the contamination requirements of the lunar habitat. This results from the need for the astronaut and any associated equipment to pass through the airlock. For instance, during the Apollo missions a significant amount of lunar material was brought into the lunar excursion module during and following each EVA. Although the astronauts attempted to remove as much lunar dust as possible from the suits with a brush before entering the airlock, a very significant amount of material remained in the folds and crevices of the EMU. In addition, the sharp edges of the dust easily interlocked with the suit outer material [3 pg. 165].

It is apparent from the requirements for a lunar surface EMU that current suit technology will need to be updated to maintain EVA capability during the long duration lunar base mission. The intensive maintenance schedule, long pre-breathe and donning time, and restricted mobility of the current EMU derived for Space Shuttle would greatly limit the lunar crew's ability to perform planned and contingency maintenance. As a result, NASA has been developing hard-suit technology for the lunar outpost as well as Space Station missions [42 pg. 91].

The hard-suit consists of a hard outer protective shell and pressure wall as opposed to the current fabric pressure suits. In the area of prevention of lunar dust contamination, the hard-suit provides a smooth and somewhat polished outer surface for reduced adhesion of the lunar dust. In addition, the lack of a fabric outer surface helps prevent interlocking of lunar dust particles to the suit surface. A potential problem with the hard-suit is the fouling of mechanical bearing seals with lunar dust. The hard-suit derives its flexibility from the bearing seals rather than the fabric joints of conventional suit technology. One possible solution is the use of disposable covers located over critical or hard to clean areas of the EMU. A problem with this alternative is the disposal of the used contaminated covers.

In addition to new hardware possibilities, some operations solutions may be helpful to prevent lunar dust contamination; specifically, minimizing the time crewmembers are exposed to the lunar environment. Although reducing the number of EVAs performed would proportionately reduce the amount of material brought into the airlock on the surface of the EMU, other reasons exist for limiting EVA time. Crew safety is the ultimate benefit of reduced EVA time, in addition to concentrating crew time on specific mission goals. As a result, advanced automation which remains in the lunar environment might be necessary to perform planned routine maintenance.

3.1.2.4 Mechanical Systems

A variety of mechanical systems will be exposed to the lunar dust environment. Equipment such as manned and autonomous lunar rovers and robotic systems will present the difficulty of keeping lunar dust from abrading critical moving parts. Fortunately, mechanical systems have been tested in previous lunar experience; for instance, the Apollo lunar rover. Beyond sealing critical moving parts, the true challenge of prevention will be in preparation for maintenance. The area of primary concern is the interfaces which must be mated and unmated during maintenance in the lunar environment. These interfaces are discussed in the following section.

3.1.2.5 Interfaces

A primary source of mechanical interfaces is derived from the maintenance of systems outside the lunar habitat. Devices such as fluid and electrical connectors, tools, and replacement parts will need to be directly interfaced with surfaces exposed to lunar dust. The current EVA Catalog contains an array of tools and equipment which have characteristics which would inhibit their use on the surface of the moon [53 pg. T-27]. Particular problems exist with threaded fasteners, pip-pins, velcro, and connectors. Equipment of these types have complex geometry and delicate mechanisms which are exposed to direct contamination with lunar dust. Extensive planning on tool designs and interfaces will be needed to permit reliable maintenance operations.

3.1.3 Prevention of Dust Accumulation on Lenses

In this section, a concept for preventing dust accumulation on the surface of lenses is explored. The concept is based on the lens cleaning problem associated with cameras and vision systems. Two of the ideas from the previous section discussing the prevention of dust on lenses are used; the automated iris and sacrificial surfaces.

A concept for a camera lens protection system is shown in Figure 3.1.3-1. The protection system consists of a cartridge which provides both a clear sacrificial protective cover and an automated iris. The clear Lexan protective cover is spooled across the lens after a sufficient amount of contamination accumulates and precludes clear vision. The automated iris on the cartridge remains closed when the camera is not in use, and is opened by activation of the camera. During operation, the cartridge is attached to the front of the camera shown in the figure. The entire system is packaged as a cartridge to facilitate maintenance by either a crewmember performing an EVA or an end-effector of a maintenance system.

3.1.3.1 Operation

The system is proposed to operate either autonomously, by a crewmember at a control station, or by an astronaut conducting an EVA.

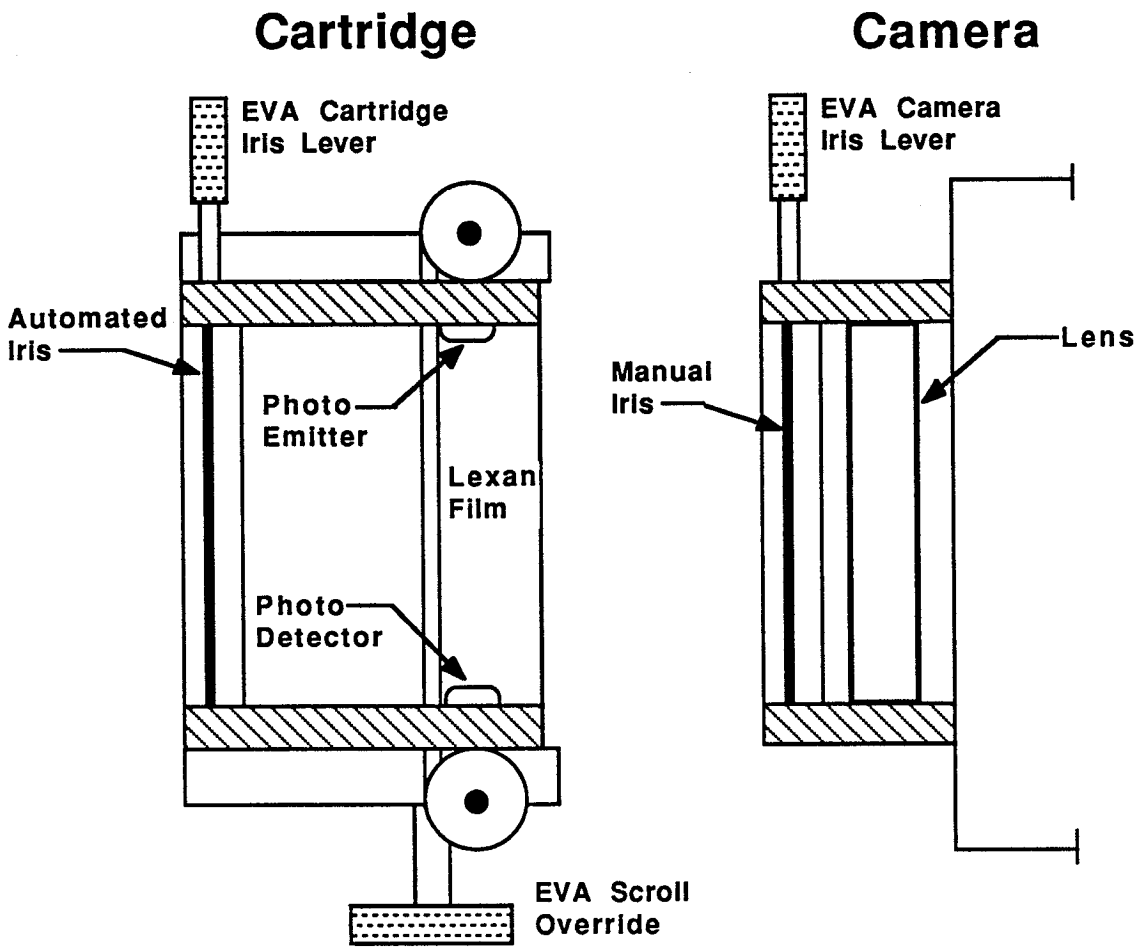

Figure 3.1.3-1: Lunar dust prevention cartridge and camera

Automatic lens covers have been used on previous space missions [13 pg. 278-287]. Essentially, the iris is provided to protect the lens and Lexan cover from lunar dust and other contaminants while the camera is not in operation. When the camera is activated the iris opens automatically. As shown in Figure 3.1.3-1, an EVA iris lever is provided to manually close the iris in the event of system failure or activity in close proximity to the camera. The iris has the disadvantage of providing an additional failure point to the camera system; as a result, it is integrated as a part of the replaceable protection cartridge.

The clear Lexan protective sacrificial surface is incorporated into a film spool system very similar to a standard 35mm still camera. Lexan was chosen due to its scratch resistance, optical properties, and proven performance on previous space missions. In addition, since Lexan does not

outgas, it does not provide its own source of contamination [4 pg. 4.108]. The sacrificial surface serves to protect the lens from direct contact with lunar dust and other contaminants. Once the protective surface itself becomes sufficiently contaminated, a new surface is scrolled into the position of the old one. This operation can be performed directly by pulling on the EVA override knob labeled in Figure 3.1.3-1, or by activation of a DC motor located in the cartridge housing. The advantage of having a motor is that the scrolling can be included as an additional function at a camera control station. A disadvantage of the motor is the additional power requirements and weight of the protection system. Current terrestrial fully automatic 35mm camera systems (with automated lens covers and flash systems) utilize a single 6V lithium battery and weigh approximately 400 grams. In the past, modified terrestrial sequence and still photographic equipment has been used on each of the Apollo missions [Apollo Summary].

3.1.3.2 Autonomous Contamination Detection

Contamination detection for lenses and optical surfaces is an area of intensive study for missions such as the Hubble Space Telescope and Space Station. Currently, the strict Space Station requirements for contamination detection are driving the state of the technology [14 pg. 138-145]. The detection of lunar dust on optical surfaces for manned lunar base may be necessary to permit some degree of autonomy for optical systems. Systems such as those needed for proposed autonomous lunar rovers may not be reachable for service by manned systems. In addition, crewmembers at control stations may not be able to easily make qualitative decisions on the level of contamination of a particular lens or optical surface. Research and applications for the detection of contamination are primarily dominated by optical devices and piezoelectrics. Measurement of thin film deposition is commonly performed in industry by determination of the reflectance and/or transmittance of coatings by the detection of light from an incident infrared source [37 pg. 10-15]. Research in piezoelectrics centers on the monitoring of surface acoustic wave mass to meet the strict Space Station contamination detection requirements [55 pg. 189-199].

In many cases, optical systems are used to provide essential and mission-critical information. In the event that a lens is obscured by lunar

dust or any other contamination, the time and resources may or may not be available to perform the maintenance action of either cleaning the lens or removing an attached sacrificial surface. In addition, the priority of crew safety and the great demand and expense of crew time should not be compromised by the critical or frequent need to clean or maintain an optical surface. As a result, a system for prevention of the obscuring of lenses by contamination should be automated to improve mission safety and reduce overall maintenance time and expense [21 pg. 74].

As shown in Figure 3.1.3-1, an infrared source and detector are proposed to provide an indication of the contamination level and an autonomous signal to scroll the sacrificial protective surface [14]. The system would operate when the camera is activated and the cartridge iris is initially closed. Light emitted from the infrared source is measured by the photodetector located opposite the emitter. Lunar dust located on the surface of the Lexan reflects a portion of the light and increases the amount of light incident on the photodetector. Once the reflectance reaches a predetermined threshold, the protective sacrificial surface is scrolled. The emitter and detector are located behind the protective surface to prevent contamination and resulting false readings.

The salient problem with the proposed system is the calibration of the emitter and detector. The threshold of each protection system would probably have to be set individually prior to launch. Power requirements for infrared emitters and detectors are very low (on the order of milliwatts), with operating temperatures of standard devices ranging from 233 K to 373 K (-110°F to +212°F) [39 pg. 3.1].

3.1.3.3 Maintenance

System maintenance is performed by direct removal and replacement of the dust prevention cartridge. As the concept in Figure 3.1.3.3-1 shows, side mounted latches are used to hold the system in place. The use of latches of this type on electrical connectors has been successfully tested with suited astronauts and telerobotics on earth [23 pg. 5].

Maintenance would begin with the crewmember on EVA manually closing the iris located in front of the lens of the camera. This iris, permanently attached to the camera, covers the camera lens during maintenance and prevents any direct contamination of the lens during

replacement of the cartridge. Next, the existing cartridge is removed by releasing the latches and directly pulling the cartridge off of the camera. A new cartridge is then placed in the position of the previous one. Finally, once the new cartridge is latched in place, the crewmember opens the iris in front of the lens. It is proposed that this maintenance operation could be performed by either an astronaut or automation system. Following replacement, it may be possible for the spent cartridge to refurbished with a new lithium source and Lexan film spool.

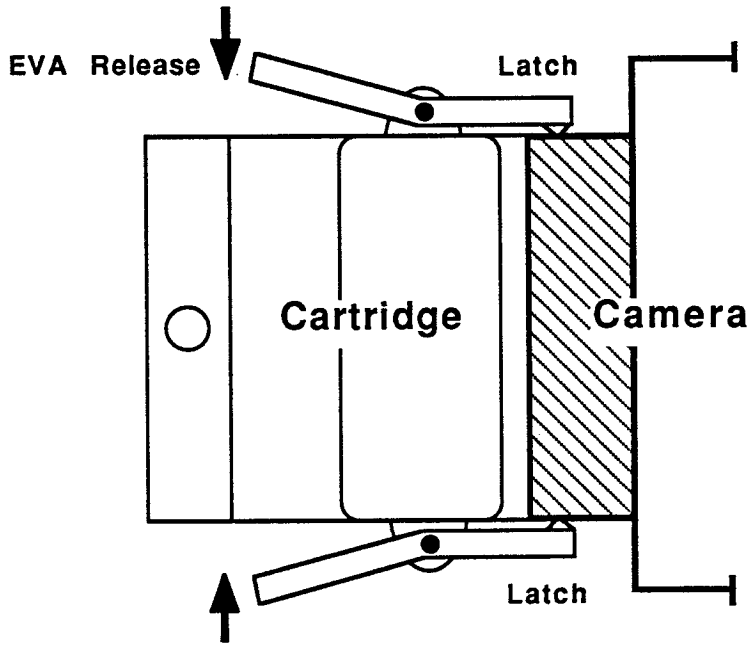

Figure 3.1.3.3-1: Prevention cartridge maintenance concept

3.1.4 Prevention Summary

In many cases, lunar operations may require the use of contamination prevention; however, the use of contamination prevention on optical lenses has some distinct disadvantages. Primarily these are, added weight and system complexity, as well as a probable reduction in optical properties. The added weight may be offset by weight savings in cleaning systems, replacement optical components, and EVA resources required for optical system maintenance. In addition, another trade-off occurs between the system complexity and crew time; an independent

system of contamination prevention requires crew attention only when the system requires replacement. The reduction in optical properties associated with the use of a sacrificial surface must be balanced with the cleaning requirements of a particular system, and the budgeting of crew time and resources.

The proposed prevention system concept utilizes readily available technology which has been tested and proven in industry and on previous space missions. In addition, the system attempts to account for the priority of crew safety and the great demand and expense of crew time.

The contamination prevention alternatives which exist for planned lunar systems constitute an extremely large body of work which will add to the operational requirements of every lunar base subsystem.

3.2 Removal

3.2.1 Electrostatic Solutions

3.2.1.1 Transportation of Dust by Electrostatics

There are many theories that explain the transportation of dust particles, but the transportation or erosion of dust by electrostatics seems to explain it best and satisfies all conditions. Erosion is assumed to be carried out in two step liberation of the particle in the transportation phase and actual transportation of the particles by the transportation mechanism.

Initially, the particles are not readily moved but when the particles are disturbed then they can be easily transported by the transportation mechanism. Only a small amount of particles are put in the transportation phase to be carried away; this mechanism of carrying only few dust particles is best explained by the electrostatic theory.

Many actions are considered responsible for the transportation of material from the lunar surface such as thermal variations,radiation pressure, forces arising from traces of gas and cycles of evaporation and condensation; but all these are considered inferior and unimportant when electrostatic phenomena is explained.

The transported dust is small in size because of degradation by meteoritic impact. The dust is also characterised by low thermal conductivity and low volumetric specific heat.

Light, X-ray radiations and particle bombardment from the sun all cause emission of secondary electrons on the surface. The emitted electrons form a thin layer near the lunar surface and are referred to as a plasma sheath. This sheath is carried away to the dark side of moon by solar wind thus forming a potential difference on the lunar surface between the sunlit and dark side.

There are two reasons for differential charging of the dust particles. First, size variations within the particles result in varying charges in the dust due to emission of electrons from the outermost orbit. This sets up strong electric fields and causes dust movement. When bombarded with electrons of sufficient energy in the form of radiation, solar radiation, the outermost orbit of an atom in an insulator can be removed, thus making the atom positively charged. When many atoms give out electrons from the outermost orbit the body overall becomes positively charged. Similarly when different particles on the lunar surface, in the same vicinity, emit varying numbers of electrons, the particles have different charges. A typical value of the energy to remove electron from the outermost orbit is about 300V. This is one of the reasons for differential charging. This electron emission sets up differential charges on the individual dust particles.

The second reason for differential charging is local topography. Grains on the high spots have more exposed area and tend to give up electrons more readily. Grains in the hollows, tend to absorb the secondary electrons from their exposed neighbours (they emit less electrons). So the ones in the hollows are at a lower positive potential than the particles on the higher level. The electric forces result from the differential charges set up, and make the dust grain move and expose a different set of surfaces. Then a new surface is set up with a new potential for movement.

Other effects are that powders are caused to migrate downhill by electron bombardment in the energy range of 200-800V [17].

The charging process may also cause electrostatic hopping and gliding of the particles resulting in particle movement. Electrostatic hopping is explained as the process in which particles acquire charge due to the differential charging by sun radiation (solar wind) and the photoelectric effect. The photoelectric effect is the phenomenon in which the metal plate

or object when exposed to radiation (X-rays or solar radiation) emits electrons after the plate or the object is heated to a certain level. This heating is measured in terms of electronvolts (eV). This emission of electrons is known as Photoelectric Emission. Two such particles may then jump apart if they are not welded, resulting in the process called electrostatic hopping. The electrostatic hopping results in particles moving downhill and thereby flattening the hills.

Another important process in surface transportation is electrostatic gliding. The concept behind this is the constant emission of electrons from the surface of moon, so the moon is at a positive potential of several volts, surrounded by a blanket of electrons, which are in transit between emission and return to the lunar surface [18].

This is similar to thermionic space charge. For an emission of 10E+11 electrons/cm**2 the space charge would be confined to about 2cm from the surface of moon.and the potential to which the moon is raised is about 3-30V [19]

So, when a small grain is lifted above the surface of moon for any reason, it may experience a large force between itself and the moon sufficient enough to cause the grain to float. If 100 electrons are discharged from the dust grain, it would experience a force of 5*10E-9 dynes. This force is large enough to cause particles of size 1*1*10 microns to float.

If any disturbance occurs on the lunar surface that disturbs dust grains, such as micrometeoritic impact or electrostatic hopping, the grains are so lifted up that they will find the potential gradient insufficient to support them anywhere except within a thin layer above the surface. If a particle is lifted to a height above 2 cm it will fall back to the surface with the electric effect unable to arrest it's momentum. But if the dust had not been lifted above 2 cm it would remain suspended in the potential field [20].

Any slope on the Moon's surface will cause a floating particle to glissade downhill. These particles will travel down the slope under the action of the gravity and continue in this frictionless descent for a short distance depending on the topography of the area. If the speed acquired is more than the electrostatic support, the particle will precipitate down and result in the smoothening of slopes and filling of small depressions.

In daytime, photoemission can produce surface potentials of only a few volts due to uniformity the of illumination and exposure to solar wind plasma. As the sunset approaches, solar wind particles are reduced greatly and illumination becomes patchy, thereby increasing the potential differences between positive (sunlit) and negative (shadowed) regions.

Electric fields of 100-1000V cm-1 may be developed around the objects. The sunlit part maintains a constant potential because low energy photoelectrons hop along the surface making it conductive. This conductor like effect concentrates positive charge towards the sunlit patch. The dark areas retain all photoelectrons striking them. This results in an intense dipole field at the sun-dark boundary. The charge density may be intensified further by the sunset effect as the freshly darkened areas become new sinks for photoelectrons, thereby increasing charge density and voltage of remaining sunlit areas.

3.2.1.2 Force Analysis of Dust Particles

Lunar soil emits photoelectrons when the soil is exposed to solar radiation. The dust particles will be levitated only when the electrostatic force exceeds the gravitational force of attraction between lunar dust and soil. Therefore from Appendix 2, the voltage is

V = Q/ C
= 4.1 *10E4 volts for the parallel plate condenser
= 1.1*10E4 volts for the hollow cylinder condenser

and the power is calculated as

Power = 0.5 * C *(V **2)
= 8.3 watts (parallel plate condenser)
= 2.1 watts (hollow cylinder condenser)

For the parallel plate electrostatic device the voltage or potential difference applied across the plates of area 0.75*0.75 is about 41000V and for the hollow cylinder type the voltage is about 11000V. If we were to consider dust particles bigger in size, then the potential difference to be applied would be greater. For different sizes the voltage applied is

different and as the size of the particles increases the voltage increases as shown in Table 1. in Appendix 2.

The voltage is very high in both the casps (parallel plate and hollow cylinder type condenser). The means of producing this electricity in great amounts by solar and fuel cells is not possible because voltages developed by such cells is on the order of 200V. Even if solar cells are used in an array the voltage developed is not as high as 11kV. The voltage developed by fuel cells is much lower than the solar cells. The power developed by the solar cells is as high as 25 kW but the voltage is not as required.

Transformers to step up the voltage can't be justified because the size is massive, the cost is very high, and losses (winding and iron) are high too. From a safety view, using 11kV voltages may be a big risk. Transportability of the transformer to the moon is also a big problem because of the massive size and weight. Disadvantages of using an electrostatic device are it covers only a small area at a time, it may become dust clogged after a long use, it requires a very high voltage, it may be unsafe, the cost of the transformer is high, size and weight adds to the cost of transport to the moon, and the source of power to be used is very complicated. Therefore from cost, safety, weight and size, transportability and portability we can infer that an electrostatic device is not feasible.

3.2.1.3 Lunar Magnetism

Strong magnetic fields are uncommon on the moon. The magnetic field strength on the moon is very low, but samples were found which show that some remnant magnetism does exist. The magnetic field strength was once very strong, a long time back (3 aeons), but now it has weakened. So the magnetic field present now is of very low intensity. The composition of the dust indicates that the iron content in the soil is too small to apply a strong magnetic field. (See Section 2.0. - Dust Characteristics) Some of the dust samples do not contain iron at all and so a magnetic device is of no use. It would remove only a portion of the particles from the optical surface. So a magnetic device is considered to be of no use in dust removal designs for the reasons stated above.

3.2.1.4 Conclusions and Further Studies

From the analysis, it can be concluded that an electrostatic device is not feasible with the data that is available. To get a better solution from the electrostatic device we must have more quantitative data about the dust charge on each individual particle. In short, the data required is charge on the dust (with respect to size). If more data becomes available then a possible solution might be seen since it is confirmed that dust has electrostatic charge.

3.2.2 Fluid Solutions

As previously discussed, the rough irregular surface contours of the dust cause strong mechanical adhesion. The jagged edges also scratch delicate surfaces when wiped away. Thus, direct mechanical dust removal can not be used on delicate surfaces without degrading the finish. This section details three areas of dust removal techniques employing fluid solutions. First, foams and gels are discussed, then liquids, and finally gases.

3.2.2.1 Foams and Gels

The first idea considered here is the use of a chemical foaming solution to lift dust particles from an optical surface. Once the dust is suspended in the foaming solution, it could be removed by blowing the foam from the surface. There are many problems implicit in this. A chemical solution would have to be found that would be strong enough to break the surface attraction forces of the lunar dust. Also, tests would have to be performed to determine if the foam would leave a residue on the surface. Another uncertainty is the concept of a foaming solution in a zero pressure atmosphere. These questions were posed to an engineer at Space Industries [1]. In his opinion that the zero pressure will cause immediate evaporation and inhibit the effects of a bubbling solution. Also, the application of foam to an optical surface would be difficult. If it was sprayed, the solution would not adhere well the optical surface. If poured over the surface, this method would be restricted to easily accessible objects only. Surfaces in hard to reach places and surfaces with irregular

contours and joints would be difficult to clean. For these reasons, foaming solutions were not pursued any further.

The next idea was an adhesive sheet. This consists of applying sheets of adhesive tape or flypaper to the optical surface. The sheets are then removed, pulling dust from the surface. This process could be repeated as many times as necessary. A major disadvantage of this idea is the disposal of adhesive sheets. Another area of concern is whether the adhesive sheets will leave a residue on the optical surface. More important is the interface with an astronaut. It would be difficult to maintain a clean adhesive strip. Some sort of backing would be needed for this purpose. Removing this backing to expose the adhesive side of the strip and applying the strip would be a tedious procedure for the gloved hand of the astronaut. Also, irregular surface contours would be difficult to clean with this method. For this reason, a variant of this idea was considered. It involves spreading a thin layer of gel on the optical surface and waiting for it to harden. The gel could then be peeled off to remove the dust. A suitable gel would need to be researched for adhesive and mechanical properties. A disadvantage of this idea is removing the hardened gel. Peeling it from the surface would again be a difficult job for the gloved hand of the astronaut.

3.2.2.2 Liquid Solutions

Two basic ideas for the removal of lunar dust were developed in the liquid domain. The first was a liquid rinse. A liquid would be sprayed over the surface to be cleaned, thus breaking the dust adhesion forces. The major problem with this alternative is the behavior of liquids in the moon's atmosphere. If cleaning was performed during the lunar day, the high temperatures and zero pressure would result in liquid evaporation. If used during the lunar night, the low temperatures and zero pressure would cause the result liquid to freeze. A frozen liquid would set up detrimental thermal gradients on the optical surface. A boiling liquid might work, but there are problems implicit in this. Some electrical components near the optical surface could get wet and be damaged. Also, the liquid might wet the astronaut's space suit after repeated cleanings. Finally, the boiling liquid could leave a residue on the surface of the optical equipment. With these problems in mind a variant fluid solution was considered.

This involved placing the object to be cleaned in an enclosed fluid bath and ultrasonically vibrating the bath. The vibrations would loosen the dust from the object and suspend them in the fluid. This is a proven technology on earth and is used in jewelry cleaning equipment. However, there are several problems with this alternate. First, it requires disassembly of any object to be cleaned. This is not a practical idea for many of the NASA cameras or observatory windows. Second, it would be difficult to clean large surface areas with such a device. Also, the fluid bath would need to be pressurized to reduce evaporation. Finally, once the object is cleaned, it would have to be reassembled without putting dust back on it, a difficult task in the lunar environment. If this alternate were implemented, it would be a relatively complex system that would be awkward to transport and difficult to automate.

3.2.2.3 Gas Solutions

Considering the problems involved with a liquid alternative, some gas solutions were considered. The cleaning method consists of blowing a compressed gas over the optical surface. This is similar to the liquid rinse in that the thrust of the gas will overcome the adhesive forces of the dust on the optical surface. The suspended dust will then be pulled to the lunar surface by the moon's gravity. There are also problems with this method. As gas exits into a zero pressure environment, it expands in all directions. Thus, not all of the gas will reach the optical surface. Also, once the dust particles are removed from the surface, they could land on the cleaned surface.

Another problem with the gas method involves thermal effects. As the gas leaves the nozzle, it rapidly expands into the zero pressure environment causing extreme temperature decreases in the gas. These decreases can cause gas condensation and icing.

A final disadvantage of any gas cleaning solution is that of environmental effects on the moon. If large quantities of gas were discharged over a long period of time, the moon's gravity could possibly contain the gas. This could result in the development of a harmful lunar atmosphere. This possibility should be considered when designing anything for the lunar base.

3.3 Alternative Design Conclusions

From the inspected alternatives, a fluid solution was chosen for detailed investigation. Although prevention must be an integral part of the design of lunar equipment, it does not remove the requirement for a lunar dust removal system. Further, mechanical cleaning alternatives such as the dust brush are inadequate due to the probable damage of the optical surface during cleaning. Electrostatics appear to be feasible yet are not practical due to the large amount of power required, large system mass, and possible safety problems. Of the alternatives utilizing a fluid for removal, the compressed gas solution was chosen due to its apparent feasibility for portability and dust removal without damage to the optical surface. As a result, section four of the report is dedicated to detailed investigation into this design alternative.

4.0 DESIGN SOLUTION

The design solution developed in this report consists of a gas cleaning method introduced in the alternative design section. Either carbon dioxide or nitrogen can be used as the cleaning medium with this design because both of these gases contain heavier molecules; as a result, their translational and rotational temperatures behave similarly in freejet expansions [25]. The calculations in this report were performed using carbon dioxide as the working gas.

The design (Figure 4.0-1) consists of two major parts: a removable pressurized gas storage tank and a handle with the gas exit nozzles. The handle is designed to be used by either an astronaut or the end-effector of a manipulator arm. In order to operate the device, it must be aimed at the surface to be cleaned within a two centimeter distance. The trigger and handle of the device are designed for the gloved hand of an astronaut. Once positioned, the trigger is pulled to allow gas to flow from the tank to the gas exit nozzles. Operation of the device by a teleoperated or autonomous system is identical to the operation by astronaut with the exception of the activation mechanism. For a machine end-effector gripping the handle,

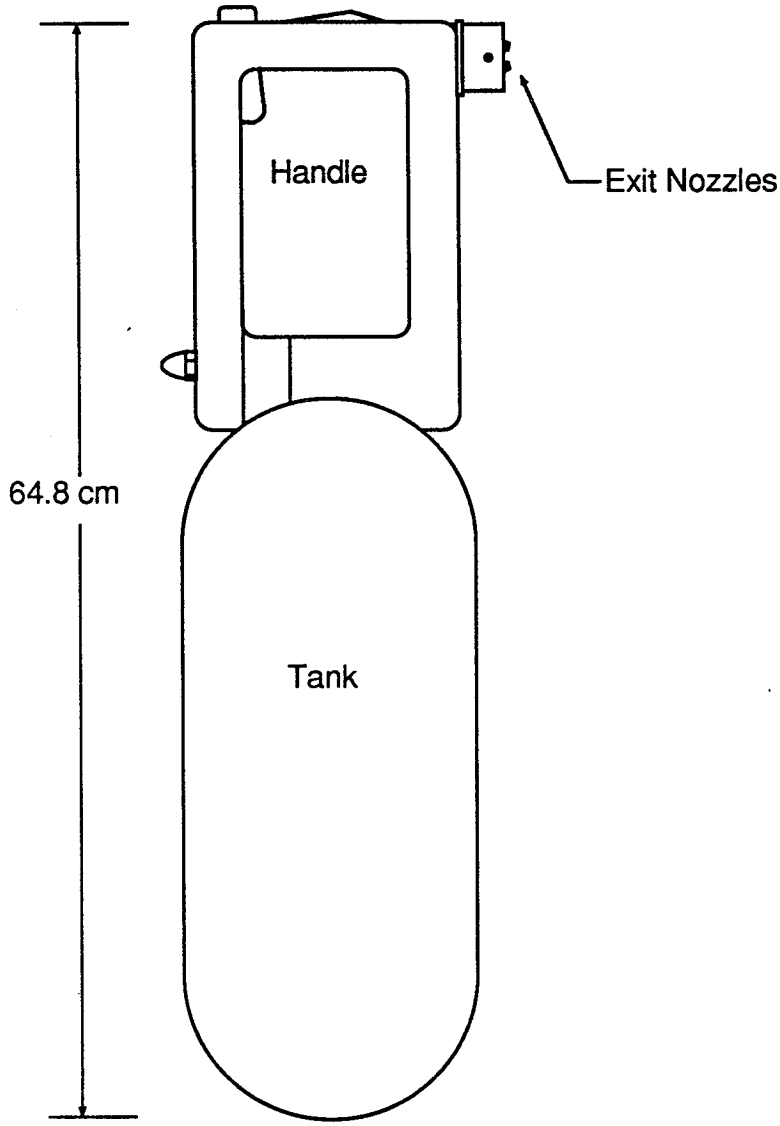

Figure 4.0-1: Design concept for gas dust removal.

rotation of the hex drive delivers gas to the exit nozzles. On the front of the handle, there are three nozzles in a triangular configuration with a common focal point. The gauge on the handle indicates the remaining tank pressure. When the gas storage tank is empty, it can be detached and recharged. The regulator in the handle regulates the 600 psi tank pressure to 1/2 psi. It can be adjusted by disassembling the handle. This is a safety feature so that the astronaut can not accidentally increase the nozzle pressure.

The tank has two hemispherical ends. The top end meshes with the curvature of the bottom of the handle. The bottom hemisphere will not allow the tank to set on a flat surface, so a tank holder was designed (Figure 4.0-2). This holder can be mounted to any convenient surface in the lunar habitat. In addition, this holder may serve as a location for the

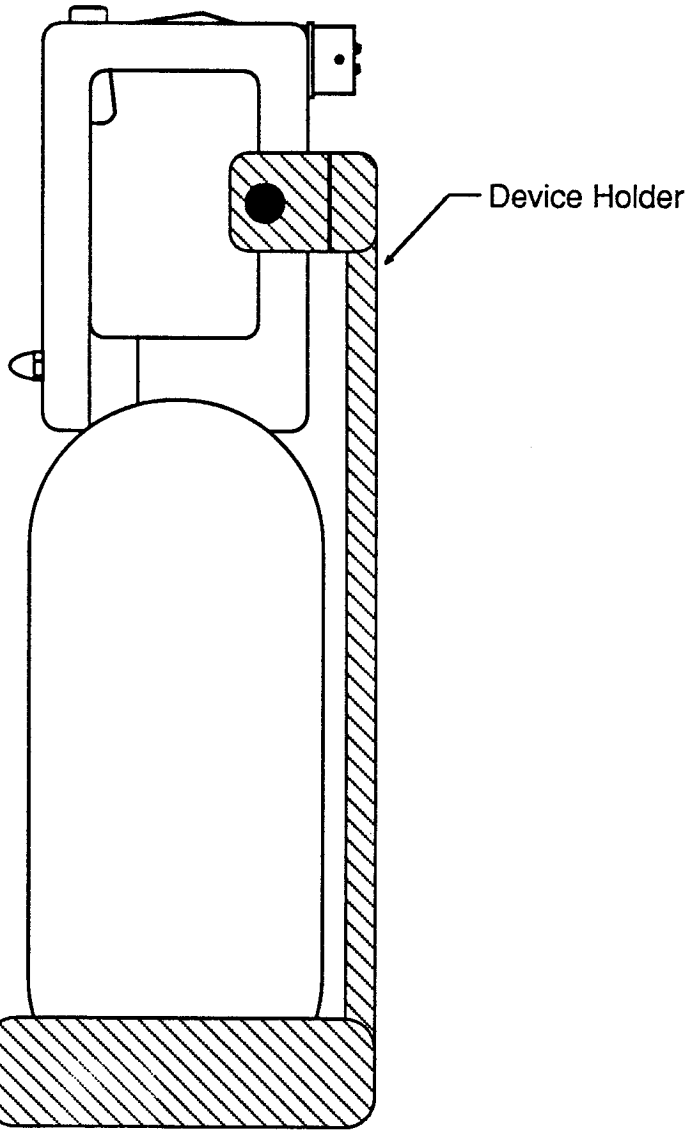

Figure 4.0-2: Design concept for a device holder.

tank during recharge, and a fixture for the tank during launch and transport to the moon. As shown in the figure, the holder consists of a cradle for the lower hemisphere of the tank and a clip for the front portion of the handle. For removal, the clip must be pulled back from the handle; for insertion, the clip automatically grips the handle as it is inserted into the holder.

The remainder of this report is divided into two major sections. First, the analytical design of the nozzle and tank will be explained. Second, the embodiment design of the handle and tank will be presented.

4.1 Analytical Design

This section describes the nozzle design. It starts at the interaction between the gas and the dust on the optical surface. From this evaluation, a thrust is determined. This thrust is then used to design the nozzle(s) so that the gas does not condense. Once the nozzle is designed, the tank pressure and volume are determined. The stagnation temperature is used as a reference state when studying properties of a flow that is assumed to be isentropic. The stagnation pressure is taken as the pressure of the gas at rest before accelerating into the nozzle (ie in tank or regulator).

4.1.1 Gas - Dust Interaction

4.1.1.1 Continuum Flow

The main idea behind this design is dust removal by gas force. This was modeled by a carbon dioxide gas plume impinging upon a flat surface with a layer of dust adhered to it. In order to model this, the amount of gas that reached the surface needed to be determined. As gas exits into a zero pressure environment, it rapidly expands. The vacuum expansion causes gas molecules to disperse in all directions, not just in the thrust direction. At some point along any streamline in this flow, there is a breakdown of the continuum flow model. The deviation from continuum flow starts to occur when a "breakdown parameter" P reaches approximately 0.05 [8 pg 681]. At values of P exceeding unity, the flow is free-molecular. For values between 0.05 and unity, the flow is in a transition regime between continuum and free molecular. This transition

zone is described by angles ranging from 30 to 45 degrees (Figure 4.1.1.1-1), measured from the flow axis [8 pg 682-685]. Thus, at angles less than 30 degrees, continuum flow can be expected. This flow is described by a fairly constant gas density [35]. The report that this information was taken from used thrust values ranging from 400 to 40000 newtons. However, the design solution presented here uses a thrust value of 0.1 newtons (as described in a later section). For this order of magnitude of thrust, continuum flow can be expected within 15 degrees of the jet axis [8 pg 686]. Therefore, the gas within a 30 degree cone was assumed to contact the optical surface. The gas outside of this cone was neglected in the dust removal calculations.

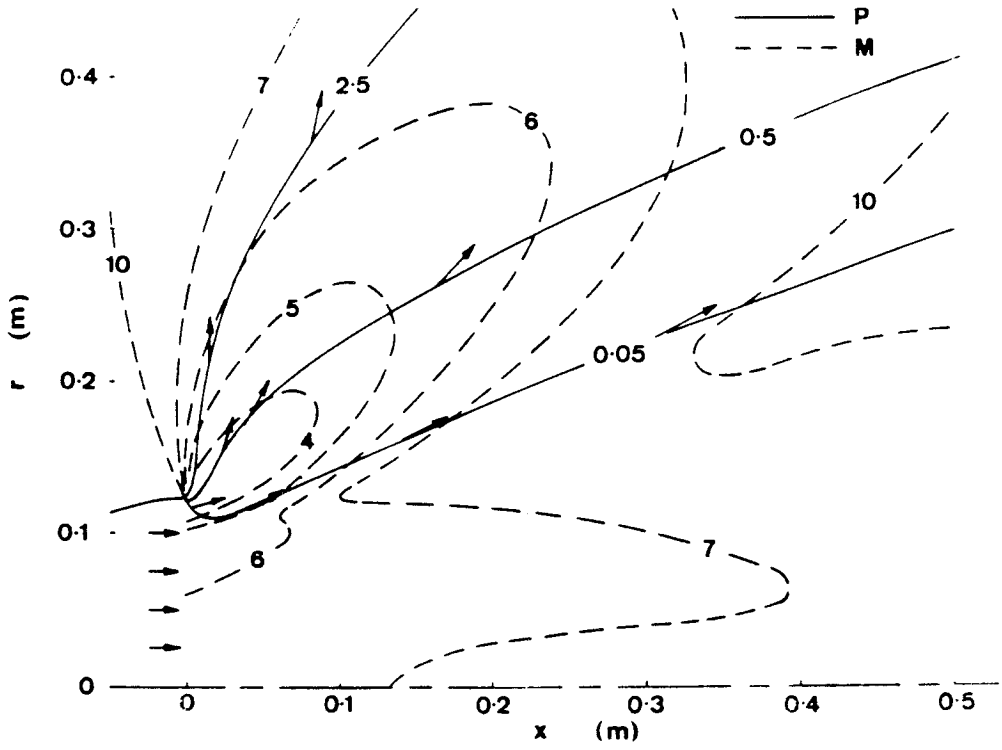

Figure 4.1.1.1-1: Continuum flow breakdown [8].

4.1.1.2 Thrust

The amount of thrust required to liberate dust from a surface was calculated by using the theoretical adhesion force per area (68.9 pascals reference) of the dust to the surface and applying an assumed coefficient of friction of unity. If the tangential force of the carbon dioxide plume striking the dust is greater than the sum of the adhesion force and the normal force of the plume, the dust will break free and be carried away bythe reflected plume lobes. This analysis is similar to one performed in a rarefied gas dynamics study [30]. The use of a coefficient of friction of unity is assumed the worst case and calculations were performed to find the optimum plume-to-surface angle. This angle was calculated to be 22.5 degrees from the surface. It should be noted that this angle is a theoretical calculation using a coefficient of friction of unity and actual in- use testing of this device will probably lead to a range of effective angles and a differing optimum angle from surface to surface.

4.1.1.3 Scattering Lobes

Depending on the gas incident angle, the gas - dust combination leaves the optical surface at various refraction angles. These angles are described by scattering lobes (Figure 4.1.1.3-1). This figure shows scattering lobes for incident angles of 30, 45, 60, and 75 degrees. As the incident angle increases, the horizontal lobe becomes more prominent. Therefore, a low incident angle will lift the dust from the surface more effectively than a large incident angle and reduce the possibility of scratching the optical surface. This corresponds well with the optimal angle of 22.5 degrees calculated previously.

4.1.2 Nozzle Design

This section introduces the empirical equations used to design a circular nozzle that will not allow the carbon dioxide to condense. The nozzle design will be separated into two areas: condensation considerations, and thrust variations.

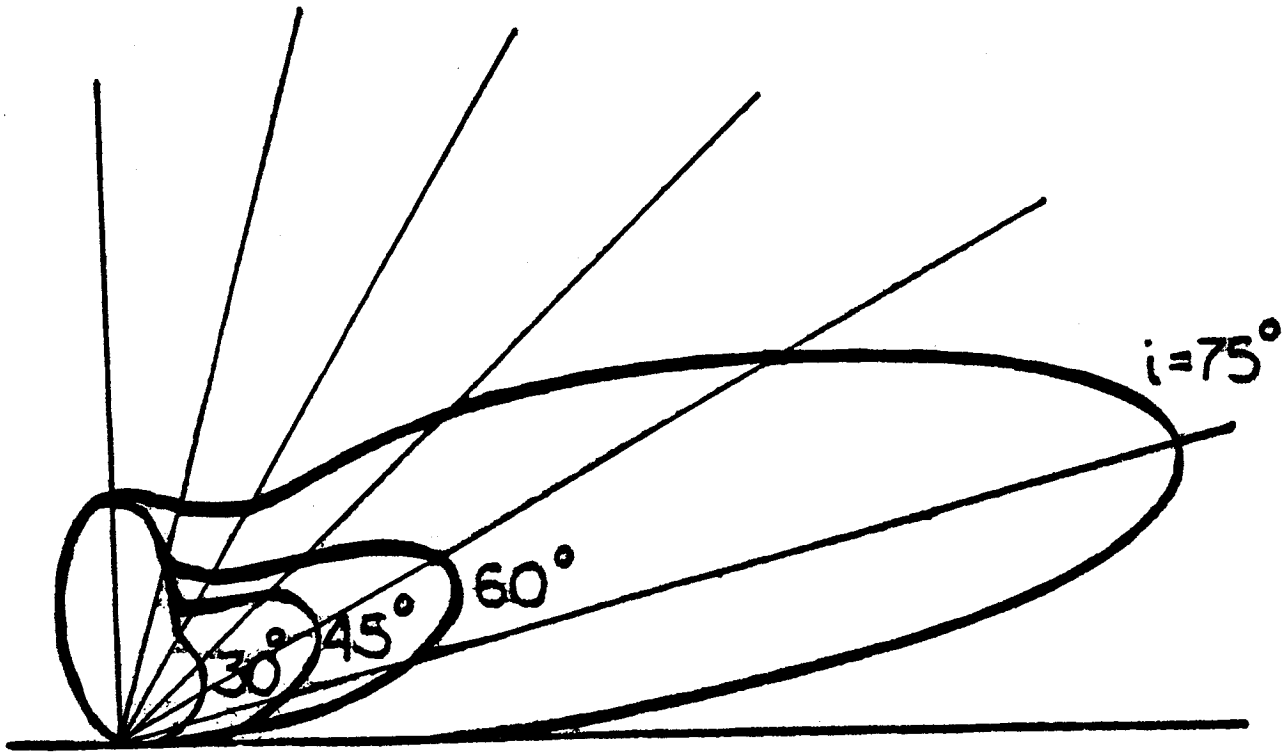

Figure 4.1.1.3-1: Scattering lobes [30].

4.1.2.1 Condensation Considerations

As the gas exits the nozzle, it expands into the zero pressure environment. In this freejet expansion, the translational temperatures of the gas decrease so rapidly that incomplete relaxation of internal energies occurs [57]. This relaxation is the cause of the continuum flow breakdown discussed in the previous section [8 pg 682]. It also leads to large temperature drops as the gas exits the nozzle. If a nozzle is not properly designed, the gas will condense when it enters the zero pressure environment. Condensation of the gas would set up large thermal gradients between the optical surface (368 K) and the solid carbon dioxide (170 K) which could damage the surface. Thus, the following section introduces a constraint that limits condensation. However, experiments have been

performed with condensed carbon dioxide as a cleaning solution [6]. The condensed carbon dioxide was blown across a mirror from two inches away and effectively cleaned a three inch diameter surface within ten seconds. However, the mirror was held at room temperature (250 K), not 360 K.

At first, a rectangular nozzle was considered. This would provide a larger exit area than a circular nozzle and the flow would have a more useful shape. However, the studies that were reviewed in the area of rectangular nozzles did not address the issue of gas condensation [7,51]. Thus, we concentrated on the design of a circular nozzle.

The first step in designing a circular jet was to choose between a divergent or convergent nozzle. When using a convergent nozzle in a zero pressure environment, choked flow will occur and the gas approaches sonic flow [47]. If a divergent nozzle is used, the flow goes supersonic. A study on freejet expansion of nitrogen stated, "Supersonic gas expansion from a high-pressure tank into low-pressure space is accompanied by a rapid drop of density and temperature, which is the cause of deviations from local thermodynamic equilibrium." [50 pg 755]. This study went on to use convergent-divergent nozzles in order to avoid gas condensation.

There are two parameters used in converging nozzles to control condensation: stagnation pressure and nozzle exit diameter. The stagnation pressure is measured at the nozzle inlet. In experiments using nitrogen and carbon dioxide, a value of 240 torr mm for the product of the stagnation pressure and exit diameter was determined as critical [31]. Above this value, condensation will occur [48]. These studies assumed an environmental temperature of approximately 300 K. When the lunar environment is much cooler than this (70 K), gas condensation will occur directly [35]. Thus, the gas cleaning apparatus can only be used during the lunar day where the lunar temperature is approximately 378 K.

4.1.2.2 Thrust Variations

Using the empirically determined constraint (on the product of stagnation pressure and nozzle exit diameter) in conjunction with an analytical relation derived from the energy equation for compressible gas flow, the exit diameter of the nozzle and the stagnation pressure were determined. The assumptions made when using the relation from the

energy equation are as follows: i.) one dimensional steady flow, ii.) perfect gas, iii.) constant specific heats, and iv.) isentropic flow. The analytical relation is, ultimately, a function of the desired thrust and stagnation temperature. (See Appendix 3.)

4.1.2.3 Nozzle Calculations

Initially, the thrust was calculated as 50 newtons. This value was based on cleaning a 100 square cm surface area. (See Appendix 4.) With this value, the nozzle diameter was calculated to be 2.8 meters with a stagnation pressure of 11.3 pascals. (See Appendix 3.) These results would obviously lead to an inappropriate nozzle. However, they do show that large surface areas must be cleaned in small sections in order to arrive at a reasonable nozzle diameter and stagnation pressure. Thus, the surface area to be cleaned was reduced to 6 square cm (1 square inch) and a thrust of 0.32 newtons was determined. (See Appendix 4.) Using this value with the previously explained equations gave a nozzle diameter of 18 mm and stagnation pressure of 1777 pascals. These values appeared more reasonable than the previous ones, but they still had a problem. The 18 mm nozzle is approximately half the width of the area to be cleaned. Since the gas expands in a 30 degree cone, this nozzle will project gas over a surface area larger than the 6 square cm. Thus, the thrust per area will decrease and the surface will not be cleaned effectively. Therefore, the 0.32 newton thrust was broken into three 0.1 newton components. This gave three separate nozzles with diameters of 6 mm and a stagnation pressure of 5300 pascals. (See Appendix 3.) The three nozzles have a common focal length of 2 cm and combined thrust of 0.3 newtons. They are symmetrically placed at 120 degree angles within a 17 mm diameter circle. This nozzle configuration will clean the 6 square cm area with an assumed 1 second burst.

4.1.2.4 Temperature Considerations

For a given thrust, the higher the stagnation temperature, the higher the exit temperature. Since the flow is choked, the exit velocity is sonic and only depends on the exit temperature. So, as the exit temperature rises, the exit velocity increases, thus, reducing the mass flow rate for the given thrust. The operating time of the device is directly proportional to

the mass of gas available divided by the mass flow rate. Therefore, the lower the mass flow rate, the less gas needed for a desired operating time. (See Appendix 7.) A plot showing the sensitivity of the operating time to the stagnation temperature for a given available mass of gas (0.39 kg, dependent on tank volume, pressure, and temperature - to be discussed in the following paragraph) and a required thrust per nozzle (0.1 N) is shown in Figure 4.1.2.4-1.

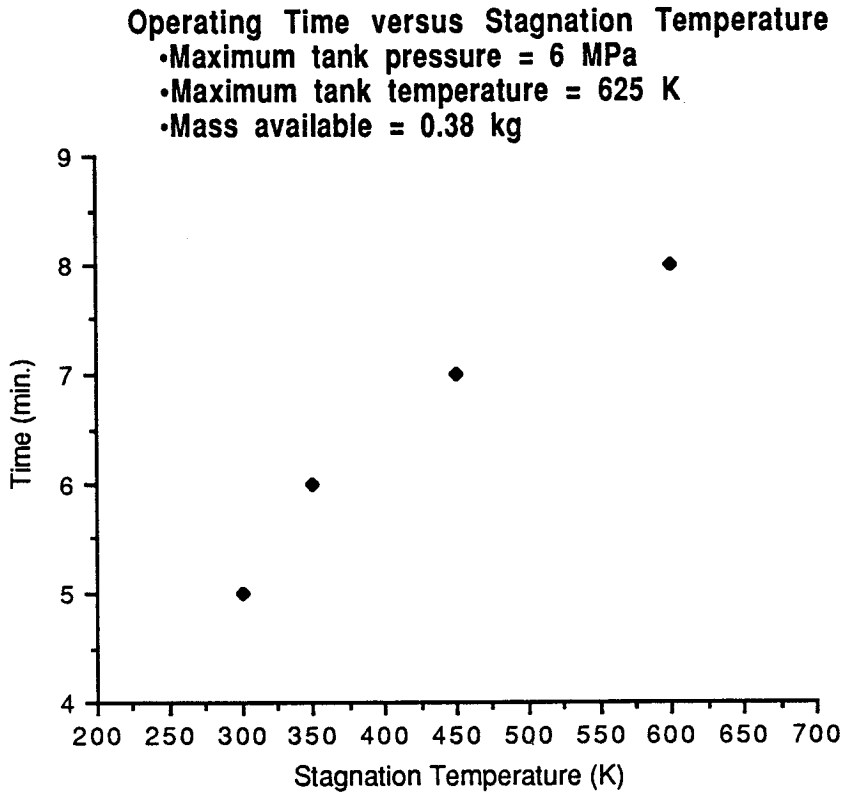

Figure 4.1.2.4-1: Operating time versus stagnation temperature

4.1.3 Tank Volume, Pressure, and Temperature

The mass of gas available for operation is dependent on the tank volume, pressure, and temperature. (See Appendix 5.) Initially, a mass flow rate (65 g/min) was determined from the thrust required and the exit velocity (calculate with an assumed temperature). A target operating time of 10 minutes was set, and thus the required mass of gas was determined

(0.65 kg). This required mass along with a tank volume of .0074 cubic meters and an assumed tank temperature were used to determine the initial pressure inside the tank. This pressure was determined to be 6 MPa. The tank volume was set as a maximum dependent on a maximum tank size (see section on tank configuration). An increase in temperature will accompany the compression of the gas, and a further increase in temperature will occur when filling the tank at this pressure. (See Appendix 6.) Holding the maximum tank pressure constant, but plugging the new tank temperature into the initial ideal gas relations (used to determine the pressure), a new mass was calculated and the corresponding operating time was compared to the target operating time of 10 minutes. Because the initially assumed tank temperature (367K) was lower than that determined from the compression and filling calculations (625 K), the mass of carbon dioxide that can be stored in the tank is less than that initially required (0.39 kg vs. the initial 0.65 kg). Although less mass can now be stored, the increase in temperature inside the tank allows for a higher stagnation temperature. The higher stagnation temperature means a higher nozzle exit velocity and, thus, a lower mass flow rate. Refer again to the plots of operating time vs. stagnation temperature (Figure 4.1.2.4-1). These plots are for an initial mass, inside the tank, of 0.39 kg and a tank temperature of 625 K. Because it has not been determined how the stagnation temperature will be affected by the pressure drops across the regulator and the environmental conditions, this plot serves to show the sensitivity of the operating time to the stagnation temperature.

The energy required to fill the tank is approximately 0.0089 kW•hrs. This is a conservative estimate assuming a 60% efficient two stage positive displacement compressor with intercooling. (See Appendix 8.)

4.2 Embodiment Design

4.2.1 Pressure Vessel Configuration

The nature of the design solution selected from the available alternatives requires the use of pressurized carbon dioxide to deliver a thrust capable of displacing dust particles from optical surfaces. The use of pressurized gas requires a vessel suitable for containing the working fluid.

The following discussion is intended to provide a method of selection for a pressure vessel configuration satisfactory for our application. The stress analysis given in Appendix 9, which this discussion is based on, makes use of standard design techniques for thin walled pressure vessels. However, this approach provides quite useful results for our immediate purpose of vessel selection.

4.2.1.1 Assumptions

The following assumptions were used to design the pressure vessel:

- Maximum value of internal pressure. - 5.8 MPa (841 Psia)
- Maximum value of internal temperature. - 390 K
- Radial component of stress in thin walled vessel is negligible.
- Stress concentration due to hole for valve is neglected.
- Fatigue, Creep, Stress Corrosion Cracking Etc... all neglected
- Wall thickness of material to be uniform throughout vessel.
- Wall thickness must be less than 10% of the vessel radius.

Three material alternatives and three vessel configurations were investigated to determine the final design. The main section of the pressure vessel is a standard right circular cylinder. Stress calculations are simple for this geometry and it is easy to fabricate. Two basic components of stress may be calculated for this section of the tank and the derivation is provided in Appendix 9. The first equation relates the tangential component of stress in a thin walled cylinder to the internal pressure and wall thickness. The second equation relates the meridional or longitudinal stress to the internal pressure and wall thickness. These equations indicate that the tangential stress developed in a thin walled vessel is twice the magnitude of the meridional stress. Therefore, the equation for the tangential component of stress should be used to compute the wall thickness of a vessel for a given internal pressure.

Design of the end closures is more complicated than the design of the tank body. Discontinuity stresses occur at the junction between the cylindrical portion of pressure vessels and the end closures or heads. Discontinuity stresses arise from the fact that the cylindrical portion of the pressure vessel does not deform in the same manner as the head when the

vessel is pressurized. Therefore, at the juncture of these components local bending and shear stresses occur to preserve the geometry of the wall. These secondary stresses are generally much smaller in magnitude than the membrane stresses which occur in the main portion of the vessel. However, they are significant and must not be neglected in the stress analysis. Consideration of the discontinuity stress is used to determine the location and magnitude of the maximum stress for each individual head configuration. Three configurations were considered based on the following criteria. First, the configuration should provide a large internal volume for a given diameter and overall length. Additionally, the configuration should produce a uniform stress distribution when pressurized so that the wall thickness will be constant. This reduces the cost and complexity of manufacturing the vessel.

4.2.1.2 Head Configuration

Three common geometries for end closures of cylindrical pressure vessels are discussed below. According to the first requirement, we wish to configure the head in such a way that the volume of the vessel is maximized for a given diameter and overall length. Based solely on this criterion, the vessel with flat heads is clearly the best selection. However, in order to satisfy the second requirement, a stress analysis of the three configurations must be performed to determine the stress distribution and efficiency of each vessel design. The following information is purely qualitative. The equations this information is based on is given in Appendix 9. [28]

First, consider the flat head vessel configuration. As mentioned previously, this configuration produces a tank with maximum volume for a given overall length and diameter. However, the flat heads behave as circular plates in bending when the vessel is pressurized [12]. Bending in mechanical elements produces an unfavorable stress distribution and is therefore used for low-pressure applications only [12]. Low pressure here is assumed to be any pressure less than or equal to 690 KPa (100 Psia). Since our particular application involves internal working pressures up to 5.8 MPa (841 Psia), this vessel configuration was eliminated from further consideration.

Next, consider the cylindrical vessel with ellipsoidal heads. Ellipsoidal heads are generally regarded as a compromise between flat and

spherical heads. The volume of a vessel with this head configuration is not as great as the volume of a flat headed vessel for a fixed overall length and diameter. However, it is more favorably stressed than the flat head vessel at all locations. The equations in Appendix 9. indicate the difference in deformation of an element at the juncture of the head and cylinder [28].

This differential deformation is what produces the discontinuity stress in the vessel. This deformation will be used for comparative purposes to the hemispherical head design presented in the following section.

The cylindrical vessel with hemispherical heads subjected to an internal pressure sustains the following stresses. In the cylindrical portion of the vessel, the tangential and meridional stresses are given by equations (1) and (2) previously derived and given in Appendix 9. The stresses in the hemispherical heads are only 50% of the maximum tangential stress developed in the cylindrical portion of the vessel. The difference in the deflection of an element in the radial direction of the cylindrical portion of the vessle and the deflection of the hemispherical head is the strain at the juncture between the head and the cylinder. (See equations 6. & 7. - Appendix 9.) This strain gives rise to the discontinuity stress present at the juncture. A hemispherically shaped head experiences less strain and consequently less stress than the ellipsoidal shaped head [28]. (See equations 8. & 5. - Appendix 9.)

4.2.1.3 Configuration Summary

The results obtained from the previous discussion may be used to determine the configuration of the vessel. Initially, the cylindrical vessel with flat heads was considered and deemed impractical because of the high internal working pressure necessary for our application.

Next, several equations were referred to which provided information regarding the strains and stresses in a cylindrical pressure vessel with ellipsoidal heads.

Finally, identical equations were provided for a pressure vessel with hemispherical heads. A comparison between these equations indicated that the hemispherical heads are more favorably stressed than the ellipsoidal heads.

The cylindrical vessel with hemispherical heads was selected as the best configuration for this application as a result of these findings. The equations for computation of the maximum stress the vessel will experience are given in Appendix 9. [12]. These equations may be rearranged to provide information on wall thickness for a given internal pressure. An allowable working stress is first computed as shown in Appendix 9. This value is then used in the determination of vessel wall thickness.

The next section addresses the material selection for the fabrication of the pressure vessel.

4.2.1.4 Material Selection

The final step in the design of the pressure vessel involves the determination of a material which will survive in the harsh lunar environment. Three materials were considered as candidates for this application based on the following criteria:

- Material must possess high strength-to-weight ratio.
- Material should have good low temperature mechanical properties.
- Coefficient of thermal expansion should be minimal.
- Fatigue strength should be high over broad temperature range.
- Must be weldable for ease of fabrication.

These requirements must be satisfied in order to ensure the device achieves its intended function.

4.2.1.5 Materials

The first material considered for pressure vessel construction was titanium. The general characteristics of titanium are as follows.

- High strength-to-weight ratio
- Low coefficient of thermal expansion relative to other high strength metals
- Good low temperature strength and toughness characteristics
- Good fatigue strength
- Excellent corrosion resistance

Ti-6AL-4V titanium alloy is a high strength, low density metal used for constructing tanks, pressure vessels, cryogenic storage vessels, airframe forgings and jet engine components [10,36]. It has good resistance to high temperature oxidation and good low temperature toughness. It can be easily welded by conventional inert gas techniques. Appendix 9 shows the stress analysis used to determine the necessary vessel thickness for an internal pressure of 5.8 MPa (841 Psia) [12]. The vessel thickness obtained from the stress analysis is .27 centimeters (.107 in.). The volume and weight calculations are also provided in Appendix 9. These values will be used for comparison purposes in the summary of this section.

The next material considered for pressure vessel construction was aluminum. The general characteristics of aluminum are as follows.

- High strength-to-weight ratio
- Can be surface hardened by anodization
- Excellent corrosion resistance
- Easily machined
- Good formability
- Nonmagnetic

The particular alloy considered for use in constructing the pressure vessel is type 6061 in the T6 temper condition. This is a wrought, heat-treatable alloy that combines the qualities of excellent corrosion resistance, ease of fabrication and good mechanical properties [10,36]. The T6 temper designation indicates that it is solution treated and furnace aged. This increases the strength without sacrificing ductility. Appendix 9. shows the stress calculation for a vessel fabricated from this alloy and subjected to an internal pressure of 5.8 MPa (841 Psia) [12]. The thickness of the vessel necessary to sustain the imposed stress is .92 centimeters (.362 in.). Because this value of wall thickness exceeds 10% of the internal vessel radius, thin walled pressure vessel equations are not applicable [28]. As mentioned previously, thin walled pressure vessel theory is based on the assumption that the wall thickness is always less than 10% of the internal radius. Thick walled theory is necessary to compute the stresses in the vessel. However, a thick walled vessel obviously has more mass than a thin

walled vessel. Since the mass of the vessel is to be minimized, this material was eliminated from further consideration.

The final material considered for pressure vessel fabrication was corrosion resisting steel. The particular alloy was 17-7 PH, which is a precipitation-hardening stainless steel with the following characteristics [10,36]:

- High strength and hardness
- Excellent fatigue strength
- Good corrosion resistance
- Readily weldable using normal procedures for stainless steels

The wall thickness of a vessel for an internal working pressure of 5.8 MPa (841 Psia) is given in Appendix 9. Volume and weight calculations are also shown and will be compared to the values obtained for the titanium vessel to determine which material should be selected for fabrication.

4.2.1.6 Pressure Vessel Summary

The results obtained from the previous discussion may now be used to determine which of the three materials is best suited for manufacturing the vessel.

Initially, aluminum was eliminated as a candidate because the strength of the particular alloy selected was relatively small. Thick walls were necessary to sustain the internal working pressure as a result of the low yield strength. The vessel was too heavy because of the thick walls and so was not considered as a viable candidate.

The results for both titanium and stainless steel are shown in Appendix 9. The wall thickness for the 17-7 PH stainless steel turns out to be the smaller of the two values. However, because it is nearly twice as dense as titanium, a vessel constructed of 17-7 PH stainless steel is 32.5% heavier than a vessel made of titanium. Additionally, Ti-6Al-4V titanium alloy has a lower coefficient of thermal expansion than 17-7 PH. This will result in smaller thermal strains when the vessel is used during the lunar day. Furthermore, titanium has better low temperature mechanical properties than stainless steel.

As a result of the aforementioned discussion, titanium is selected as the material for fabrication of the pressure vessel. In addition to the previous remarks concerning materials it should be mentioned that cost was a factor in the selection process. The titanium vessel will be more expensive to fabricate because the raw material cost more. However, the cost to launch one pound of payload to the moon is approximately $50,000. The extra cost of building the vessel out of titanium is easily justified under these circumstances.

4.2.2 Handle Configuration

The aluminum handle shown in cross-section in Figure 4.2.2-1 is based on conceptual and existing tool designs for astronaut and machine end-effector compatibility. For the astronaut, the handle grip was patterned after standard EVA handles which have been specifically developed for gripping with an EMU glove. The dimensions of the handling interface were determined from an example handle shown in the Man-Systems Integration Standards [33]. Activation of the nozzles is accomplished by pulling the trigger mounted in a pistol grip fashion on the handling interface. Trigger activation was chosen due to existing tools in the EVA Catalog which utilize this mechanism [53]. However, a safety lock switch is provided on the surface of the handle to prevent inadvertent activation of the trigger. The simple two position switch displays a red color when the trigger is armed, and a green color when the trigger is disabled.

Compatibility with the end-effector of automated systems is attained by the incorporation of a hex drive into the lower portion of the EVA handle. Current designs for end-effector interfaces as shown in the Robotic System Integration Standards include the use of a parallel jaw gripper with a central socket drive [23]. This robot gripper developed for use on Space Station has the designed capability for gripping standard EVA handles. The hex drive is utilized because activation of the trigger mechanism may otherwise require development of a special end-effector. As a result, the end-effector activates the nozzles by a rotation of the hex drive. Consequently, the hex drive is independent of the EVA safety lock switch provided for the trigger mechanism.

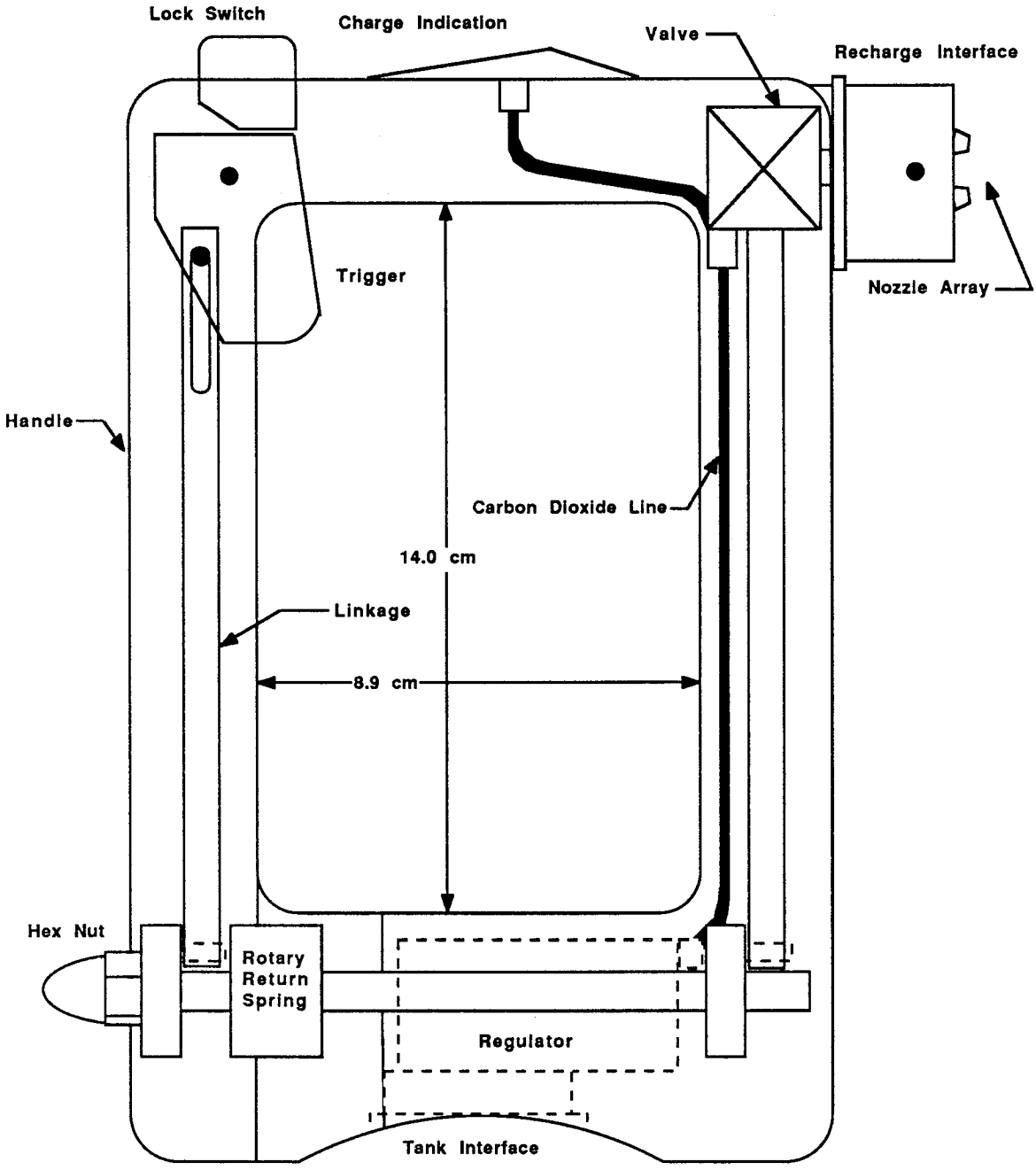

Figure 4.2.2-1: Handle configuration

Other features of the handle include the charge indicator, nozzle array, recharge connector, and tank interface. The charge indicator presents direct viewing of tank pressure at steady-state and during discharge and recharge of tank pressure. The indicator is mounted on the top face of the handle to allow direct viewing by crewmembers and machine vision systems. The nozzle array is mounted to a standoff on the upper front face of the handle. The location of the array provides a direct view of the alignment and location of the array relative to a targeted cleaning area. In addition, the standoff for the array is used as a recharge connector. The connector shown is the male portion of the standard EVA Wing Tab connector from the EVA Catalog [53]. When connected to an active charging source, filling of the tank commences when the trigger is pulled. The bottom of the handle is contoured to fit the radius of the tank, and includes a threaded tank interface.

4.2.2.1 Operation

For operation by an astronaut during an EVA, the safety lock switch located on the upper surface of the handle must be moved to the "ON" position. This switch prevents inadvertent actuation of the gas cleaning device. Next, the nozzle array is aimed directly at the surface to be cleaned. The nozzles must be within two centimeters of the targeted surface in order to get the full benefit of the gas burst. Once positioned, the trigger is pulled to allow gas to flow from the tank to the nozzle array. Maximum efficiency is obtained by the use of short and well positioned gas bursts.

Operation of the device by an teleoperated or autonomous system is identical to the operation by astronaut with the exception of the activation mechanism. For a machine end-effector, rotation of the hex drive delivers the gas to the nozzle array. The hex drive which is mounted central to the robot grip point does not require the safety lock switch because rotation of the hex drive is accomplished by a teleoperated or autonomous end-effector with safety lock systems of its own.

5.0 OVERALL CONCLUSIONS AND RECOMMENDATIONS

This device was designed to clean delicate optical surfaces. However, upon design completion, it appears that the gas apparatus can be used to clean other objects. The three nozzle design delivers 0.3 newtons of thrust at 5120 pascals (3/4 psi) with a mass flow rate of 48 g/min. If the nozzles were changed to a single smaller diameter nozzle, the thrust per area would increase and the device could clean a spacesuit or painted surfaces. However, for scratch resistant surfaces or for those surfaces whose integrity is not critical, a brush can be used. NASA currently has a brush for this purpose in their EVA Catalog [53]. Studies need to be performed to determine which of these cleaning methods is more effective.

The gas cleaning device also has other possible uses. Since carbon dioxide is an inert gas and the device operates at a relatively low thrust, it could be used as a fire extinguisher. Another possibility involves the storage tank. It could be disconnected from the handle and used to transport gases from the lunar habitat to remote sites.

A final consideration is areas of further study. The nozzle configuration is constrained by condensation effects. As technology progresses, slit orifices need to be considered because they might deliver a larger thrust per area than a circular orifice.

Also, two analyses concerning the tank need to be considered: fatigue and thermal. When the tank is in the lunar habitat, it is at approximately atmospheric pressure. As it is brought into the lunar environment, the low pressure induces a stress in the tank. Over time, this cyclic stress might cause fatigue damage to the tank. Additionally, there are stresses in the tank due to adverse thermal effects. The temperature difference between the shadow side and the light side of the tank can be as high as 250K. This causes thermal cycling of the gas in the tank and thermal stresses in the tank walls. A thermal insulation is suggested to overcome this problem on a temporary basis. However, further research might suggest that a heating/cooling system is needed for the tank.

Another important area of the design of the dust removal device, which has not been covered by this project, is a failure modes effect analysis. It is important to determine the 'weakest link' of the design, and the effects of failures of each component on the overall system. Such an

analysis will affect the detailed design/selection of individual components such as nozzles, switches, valves, seals, connectors, regulator, and linkages. The failure modes and probabilities of each component are directly related to the reliability of the device.

A final consideration is the build-up of a gas atmosphere on the moon (suggested earlier). The gas cleaning device disperse only small amounts of gas during each use. Considering the size of the moon in relation to this, it does not appear to present a problem. However, this concept should be remembered when designing anything for use on the lunar surface.

A possible disadvantage of the device lies in the incident - refraction angles discussed earlier. At large incident angles, the refraction lobes approach a horizontal scattering of the gas. This could drag dust along the optical surface, marring its finish. When cleaning small objects with large curvatures, the astronaut will not be able to maintain a small incident angle over the whole surface. Tests need to be performed to determine the amount of surface degradation due to dust particles travelling across the surface.

Another disadvantage of the device is related to dust suspension. The gas lifts the dust from optical surfaces and suspends it in the lunar environment. Some of this spaceborne dust could land on the cleaned surface. This problem will be more severe on horizontally mounted surfaces than on vertical surfaces. A possible solution to this problem would be to attach a flexible extension to the nozzle end. This extension would fit around the surface to be cleaned; thus channeling the gas - dust mixture away from the cleaned surface.

REFERENCES

1. Allen, J., Bergeron, D., Humble, R., Space Industries, personal communication, March 12, 1991.

2. American Geological Institute, Dictionary of Geological Terms. Anchor Press, Garden City, N. Y., 1976.

3. Apollo 11 Mission Report, NASA Special Publication 238, NASA Manned Spacecraft Center, 1971, p. 165.

4. Apollo Program Summary Report, NASA Lyndon B. Johnson Space Center, Houston, Texas, JSC-09423, April 1975, pp. 4.108-4.115.

5. Avallone, E. A., Baumeister III, T., (Ed.), Marks' Standard Handbook for Mechanical Engineers. McGraw-Hill Book Co., N.Y., 1987.

6. Benninghoven, Kim A., "Effects of Particulate Contamination on Optical Solar Reflectors," Proceedings of the International Society for Optical Engineering, Optical System Contamination: Effects, Measurement, and Control, May 19-22, 1987, Vol. 777, pp. 91-96.

7. Beylich ,A. E.,"Nonequilibrium effects in plane jets ", Progress in Astronautics and Aeronautics. Vol. 74, pt. 2, Ed. M. Summerfield, AIAA, New York, 1980.

8. Bird, G. A., "Breakdown of continuum flow in freejets and rocket plumes", Progress in Astronautics and Aeronautics. Vol. 74, pt. 2, Ed. M. Summerfield, AIAA, New York, 1980.

9. Brown, G., et. al., The Moon, A New Appraisal - From Space Mission and Lab Analysis. University Press, Cambridge, 1977.

10. Budinski, Kenneth G., Engineering Materials: Properties & Selection, Reston Publishing Company, Inc., 1979

11. Buresch, M., Photovoltaic Energy Systems. McGraw-Hill Book Company, 1983.

12. Burr, Arthur H., Mechanical Analysis and Design, Elsevier Science Publishing Co., Inc., 1982

13. Bush, J., et. al., "Hubble Space Telescope Protective Cover System," Proceedings of the International Society for Optical Engineering, Photovoltaics for Commercial Solar Power Applications, Sept. 18-19, 1986, Vol. 706, pp. 278-287.

14. Carosso, J. P., "Space Station Users Contamination Requirements," Proceedings of the International Society for Optical Engineering, Photovoltaics for Commercial Solar Power Applications, Sept. 18-19, 1986, Vol. 706, pp. 138-145

15. Carr, M. H., Proudfoot, S. J., "Debris on the Surveyor 3 mirror", Analysis of Surveyor 3 material and photographs returned by Apollo 12. National Aeronautics and Space Administration, Washington D. C., 1972.

16. Carroll, W. F., Blair, P. M., Hawthorne, Jacobs, S., Leger, L., "Returned Surveyor 3 hardware: Engineering results", Analysis of Surveyor 3 material and photographs returned by Apollo 12. National Aeronautics and Space Administration, Washington D. C., 1972.

17. Criswell , D., Pellizari, M., "Lunar dust transport by photoelectric charging at sunset", Proceedings Lunar and Planetary Science Conference, 9th. Volume 3, Pergamon.

18. Criswell , D., "Lunar Dust Motion ", Proceedings of Lunar Conference, 3rd. Vol 3, MIT Press,1972.

19. De, B.R., Criswell, D. R., "Part I :Generation of Intense Electric Fields in Photo Emitting Areas of Lunar Sunset Terminator Region", Journal of Geophysical Research. Vol. 82, 1977

20. De,B.R.,and D.R.Criswell, "Part II :Supercharging at the Progression of Sunset" Journal of Goephysical Research. Vol. 82,1977

21. Fisher, William F., and Price, Charles R., Space Station Freedom External Maintenance Task Team: Final Report, NASA Lyndon B. Johnson Space Center, Houston, Texas, July 1990, Vol. 1, Part 1, p. 74.

22. Flood, Dennis J., "Space Solar Cell Research: Problems and Potential," Proceedings of the International Society for Optical Engineering, Photovoltaics for Commercial Solar Power Applications, Sept. 18-19, 1986, Vol. 706, pp. 34-39.

23. Fluid and Electrical Connector Evaluation, Test Report, NASA Crew and Thermal Systems Division, NASA Lyndon B. Johnson Space Center, Houston, Texas, JSC-24655, July 1990, p. 5.

24. Franklin, A. C., Franklin, D. P., The J& P Transformer Book. Butterworths, London,1983.

25. Godfried, H. P., Silvera, I. F., Van Straatem, J., "Rotational temperatures and densities in H_2 and D_2 freejet expansions", Progress in Astronautics and Aeronautics. Vol. 74, pt. 2, Ed. M. Summerfield, AIAA, New York, 1980.

26. Gold, T., "Processes on the Lunar Surface", Symposium International Astronautical University at Pulkhova Observatory Leningrad. no.14, Ed. Kopal, Z., Mikhailov, Z. K., Academic Press, 1962

27. Grard , R. J. L., "Horizon glow and Motion of Lunar Dust ", Photons and Particle Interaction with Surfaces in Space. D. Reidel Publishing Co.,

28. Harvey, John F., Theory and Design of Modern Pressure Vessels, 2nd Edition, Van Nostrand Reinhold Company, 1974

29. Howell, J. R., Buckius, R. O., Fundamentals of Engineering Thermodynamics. McGraw-Hill Book Co., N. Y., 1987.

30. Hurlbut, F. C., "Particle surface interaction in the orbital context: A survey", Progress in Astronautics and Aeronautics. Vol. 116, Ed. M. Summerfield, AIAA, Washington D. C., 1988 .

31. Karelov, N. V., Sharafutdinov, R. G., Zarvin, A. E., "Rotational relaxation in nitrogen freejets in the transition regime", Progress in Astronautics and Aeronautics. Vol. 74, pt. 2, Ed. M. Summerfield, AIAA, New York, 1980.

32. Lataire, L., "Optical Sensors for Factory Automation," Proceedings of the International Society for Optical Engineering, In Situ Industrial Applications of Optics, June 25-27, 1986, Vol. 672, pp. 26-40.

33. Man-System Integration Standards, Rev. A, Vol. 11, NASA-STD-3000, NASA Lyndon B. Johnson Space Center, Oct. 1989, pp. 48-55.

34. Marvin, Dean C. and Hwang, Warren C., "Contamination Effects of GPS Navstar Solar Array Performance," Space Photovoltaic Research and Technology, NASA Conference Publication 3030, April 19-21, 1988, pp. 301-305.

35. Mikami, H., Saito, T., "Flow properties in a freejet of a binary gas mixture incident on a cold plate", Progress in Astronautics and Aeronautics. Vol. 74, pt. 2, Ed. M. Summerfield, AIAA, New York, 1980.

36. Metallic Materials and Elements for Aerospace Vehicle Structures, Mil-Hdbk-5E,Department of Defense, 1 June 1987.

37. Netterfield, R. P., Martin, P. J., and Muller, K.-H., "In-situ Optical Monitoring of Thin Film Deposition," Proceedings of the International Society for Optical Engineering, In Process Optical Measurements, Sept. 22-23, 1988, Vol. 1012, pp. 10-15.

38. Nickle, N. L., Carroll, W. F., "Summary and Conclusions", Analysis of Surveyor 3 material and photographs returned by Apollo 12. National Aeronautics and Space Administration, Washington D. C., 1972.

39. Optoelectronics Data Book: Infrared, Imaging, and Visible Products, Texas Instruments, 1983-1984, p. 3-1 and p. 5-1.

40. Peterson, R. V., Bowers, C. W., "Contamination removal by CO_2 jet spray", Optical System Contamination: Effects, Measurement, Control II. Ed. A. P. Glassford, SPIE - The International Society for Optical Engineering, Bellingham, Washington, 1990.

41. Podnieks, Egons R., Siekmeier, John A., Mining Technology for Lunar Resource Utilization , U.S. Department of the Interior Bureau of Mines, July 1990

42. Reinhardt, A., "AX-5 Advanced Space Suit Design Overview," Third Annual Workshop on Space Operations, Automation, and Robotics (SOAR' 89), NASA Lyndon B. Johnson Space Center, Houston, Texas, NASA Conference Publication 3059, July 25-27, 1989, p. 91.

43. Rennilson, J., Holt, H., Moll, K., "Changes in optical properties of the Surveyor 3 camera", Analysis of Surveyor 3 material and photographs returned by Apollo 12. National Aeronautics and Space Administration, Washington D. C., 1972.

44. Robertson, D. M., Gafford, E. L., Tenny, H., Strebin Jr., R. S., "Characterization of dust on clear filter from returned Surveyor 3 television camera", Analysis of Surveyor 3 material and photographs returned by Apollo 12. National Aeronautics and Space Administration, Washington D. C., 1972.

45. Rogers, A. W., Lengrand, J., "Thruster plume impingement forces measured in a vacuum chamber and conversion to real flight conditions", Progress in Astronautics and Aeronautics. Vol. 116, Ed. M. Summerfield, AIAA, Washington D. C., 1988 .

46. Sagitov et al, Lunar Gravimetry, etc...

47. Saad, M. A., Compressible Fluid Flow. Prentice Hall, Englewood Cliffs, New Jersey, 1985.

48. Schabram, R. G., Beylich, A. E., Kudriavtsev, E. M., "Experimental investigation of CO_2 and N_2O jets using intracavity laser scattering", Progress in Astronautics and Aeronautics. Vol. 117, Ed. M. Summerfield, AIAA, Washington D. C., 1988.

49. Scott, R. F., Zuckerman, K. A., "Examination of the Surveyor 3 surface sampler scoop", Analysis of Surveyor 3 material and photographs returned by Apollo 12. National Aeronautics and Space Administration, Washington D. C., 1972.

50. Sharafutdinov, R. G., Skovorodko, P. A., "Rotational level population kinetics in nitrogen freejets", Progress in Astronautics and Aeronautics. Vol. 74, pt. 2, Ed. M. Summerfield, AIAA, New York, 1980.

51. Sreekanth, A. K., Davis, A., "Rarified gas flow through rectangular tubes: Experimental and numerical investigation", Progress in Astronautics and Aeronautics. Vol.116, Ed. M. Summerfield, AIAA, Washington D. C., 1988.

52. Taylor,S.R., Planetary Science, A Lunar Perspective, A Post Apollo Review. Pergamon Press, N. Y., 1975.

53. Trevino, R. C., et. al., EVA Catalog: Tools and Equipment, JSC-20466, Rev. A, NASA Lyndon B. Johnson Space Center, Houston, Texas, April 1988, p. T-27.

54. Van Wylen, G. J., Sonntag, R. E., Fundamentals of Classical Thermodynamics. John Wiley and Sons, N. Y., 1985.

55. Wallace, Donald A., et. al., "Tests of a 200MHz Surface Acoustic Wave Mass Monitor in a Space Environment," Proceedings of the International Society for Optical Engineering, Optical System Contamination: Effects, Measurement, and Control II, July 10-12, 1990, Vol. 1329, pp. 189-199.

56. Williams, R. J., Jadwick, J. J., Editors, NASA Reference Publication 1057: Handbook of Lunar Materials. NASA Scientific and Technical Office, 1980.

57. Yamazaki, S., Taki, M., Fujitani, Y., "Rotational and vibrational relaxation in freejet expansions of CO2 at stagnation temperatures ranging from 300 K to 1300 K", Progress in Astronautics and Aeronautics. Vol. 74, pt. 2, Ed. M. Summerfield, AIAA, New York, 1980.

APPENDIX 1

NASA/USRA Project 1990-V

Design of Equipment for Lunar Dust Removal and Capture

February 22, 1991

	Function
D	1. Remove accumulated dust from all surfaces, including:
	1.1 External Mobility Unit (EMU) - suit
	1.2 Optics
	1.3 Mechanisms
	1.4 Thermal radiators
D	2. Remove without damage to polished or delicate surfaces
D	3. Remove without interference with mechanism function
	4. Removal outside pressurized volumes:
W	4.1 EV Astronaut not required for operations - remote systems
D	4.2 Compatible for Astronaut or robotic operations
	5. Removal inside pressurized volumes:
D	5.1 Removal of dust from atmosphere as well as surfaces
W	5.2 Disposal outside the pressurized volume - with other waste
W	6. Verification of cleaning function or completeness
W	7. Prevention of dust accumulation:
	7.1 Prevent attachment of dust to surfaces
	7.2 Protective covers will not interfere with mechanism function
	7.3 Contain the dust to prevent reaccumulation
	Operation
D	1. X year life-cycle (Long)
D	2. Reliability:
	2.1 Easily maintained by an Astronaut or robotic system
	2.2 Redundancy in any task critical mechanism
	2.3 Dual redundancy in any safety or mission critical mechanism
	2.4 Fail safe
D	3. Low power - energy source and transmission
W	4. Passive thermal system
D	5. Low system mass
	Conditions
	1. Outside pressurized volumes:
	1.1 Temperature gradient (-276 to 232 F)
	1.2 1/6 G
	1.3 No atmosphere
	1.4 Dust, rock (Dust: 40-130 microns, 70 average, Large surface/volume)
	1.5 Contaminants due to man's presence
	1.6 External power sources
	1.7 External thermal sources
	1.8 Materials
	1.9 Radiation
	2. Inside pressurized volumes:
	2.1 Internal pressure (10.2psia ?)
	2.2 Atmosphere - composition, including other contaminants
	2.3 Parts per million of dust acceptable

2.4 Power sources
2.5 Architecture
2.6 Materials

3. Equipment to be cleaned:
   3.1 Surface temperature gradient
   3.2 System dynamics
   3.3 Surface properties
   3.4 Location: local or remote
   3.5 Thermal equipment and optics may be special cases
   3.6 Covers, standoffs, or shielding
   3.7 Seals and lubricants

Ergonomic

1. Safe for manned or unmanned systems internal or external to the pressurized volumes
2. Man systems requirements base - Manned Systems Integration Standards (MSIS)
3. Robotic system requirements base - Robotic System Integration Standards (RSIS)

Getting it there

1. Launch mass
2. Launch loads - landing loads, emergency return
3. Packaging for launch and unloading on the surface
4. Assembly by Astronaut or robotic systems
5. Cold soak - journey from the earth to the moon, no power, no thermal

Manufacture

1. One-off items with detailed system to inspect full functionality prior to launch
2. Cost: Insignificant relative to delivery costs
3. Mock-ups and test articles required prior to delivery of the final item

The charge on the dust particle is

$$Q = \pi (A^2) (5.5 \times 10^5 \text{ electrons})/\text{cm}^2$$

where

A = size of the particle in microns

= 1 micron (1×10^{-6} m).

1 electron = 1.609×10^{-19} C

$$\therefore Q = \pi (1 \times 10^{-6})^2 (5.5 \times 10^5 \times 1.609 \times 10^{-19}) \text{ C}$$

$$= 2.7 \times 10^{-21} \text{ C}.$$

The force between the dust particle and electrostatic plate must excede the force between dust particle and optical surface.

The force between dust particle and optical surface is assumed to be $F = 1 \times 10^{-10}$ N.

$$\therefore \frac{1}{4\pi\epsilon_0} \frac{Q q}{r^2} = F$$

where ϵ_0 = permissivity = 8.85×10^{-12} $C^2/N\,m^2$

$$\therefore \frac{1}{4\pi\epsilon_0} = K = 9 \times 10^9 \text{ N m}^2/\text{C}^2$$

$$\therefore \frac{2.7 \times 10^{-21} \times q \times 9 \times 10^9}{(1 \times 10^{-2})^2} = 1 \times 10^{-10} \text{ N}$$

where r = distance of the dust particle from electrostatic plate

$= (1 \times 10^{-2})$ m.

$\therefore q = 4.1 \times 10^{-4}$ C is the charge on the electrostatic plate.

Consider parallel plate and hollow cylindrical condenser.

i) $C = \frac{A \epsilon_0}{d}$ for parallel plate type condenser

where A = area of the plates

d = distance between them.

$A = 0.75 \times 0.75$ m^2

$d = 0.5$ m.

$\therefore C = 9.95 \times 10^{-9}$ F

ii) $C = \frac{2\pi L \epsilon_0}{\ln(b/a)}$ for hollow cylindrical type condenser

where L = Length of cylinder = 1m

b = inner diameter of outer cylinder

$= 0.5$ m

a = outer dia. of inner cyl. = 0.1m

$\therefore C = 3.455 \times 10^{-8}\ F$

$\therefore$ Voltage required for

(i) parallel plate condenser is

$$V = \frac{Q}{C} = \frac{4.1 \times 10^{-4}}{9.95 \times 10^{-9}} = 4.1 \times 10^{4}\ V.$$

ii) hollow cylindrical type condenser is

$$V = \frac{Q}{C} = \frac{4.1 \times 10^{-4}}{3.455 \times 10^{-8}} = 1.1 \times 10^{4}\ V.$$

So the Power requirements for the different condensers is

$$P = \frac{1}{2} C V^2$$

$= 8.3\ W$ (parallel plate type)

$= 2.1\ W$ (hollow cylinder type)

Calculations

	1	2	3	4
a (size) (10^{-6} m)	1.0	2.0	3.0	4.0
Q coulombs	2.7×10^{-21}	1.11×10^{-20}	2.5×10^{-20}	4.4×10^{-20}
q/ coulombs	4.1×10^{-4}	5.1×10^{-4}	4.4×10^{-3}	1.25×10^{-2}
Force Newtons	1×10^{-10}	5×10^{-10}	1×10^{-9}	5×10^{-9}
Capacitance (// plate) Farads	9.95×10^{-9}	9.95×10^{-9}	9.95×10^{-9}	9.95×10^{-9}
Capacitance (hollow cyl) Farads	3.45×10^{-8}	3.45×10^{-8}	3.45×10^{-8}	3.45×10^{-8}
Voltage V (// plate)	4.1×10^{4}	5×10^{4}	4.5×10^{5}	5.25×10^{5}
Voltage V (hol. cyl)	1.1×10^{4}	1.4×10^{4}	1.2×10^{5}	3.6×10^{5}
Power W (// plate)	8.35	12.41	963.1	1057.7
Power W (hol cyl)	2.08	3.35	248.4	2235.87

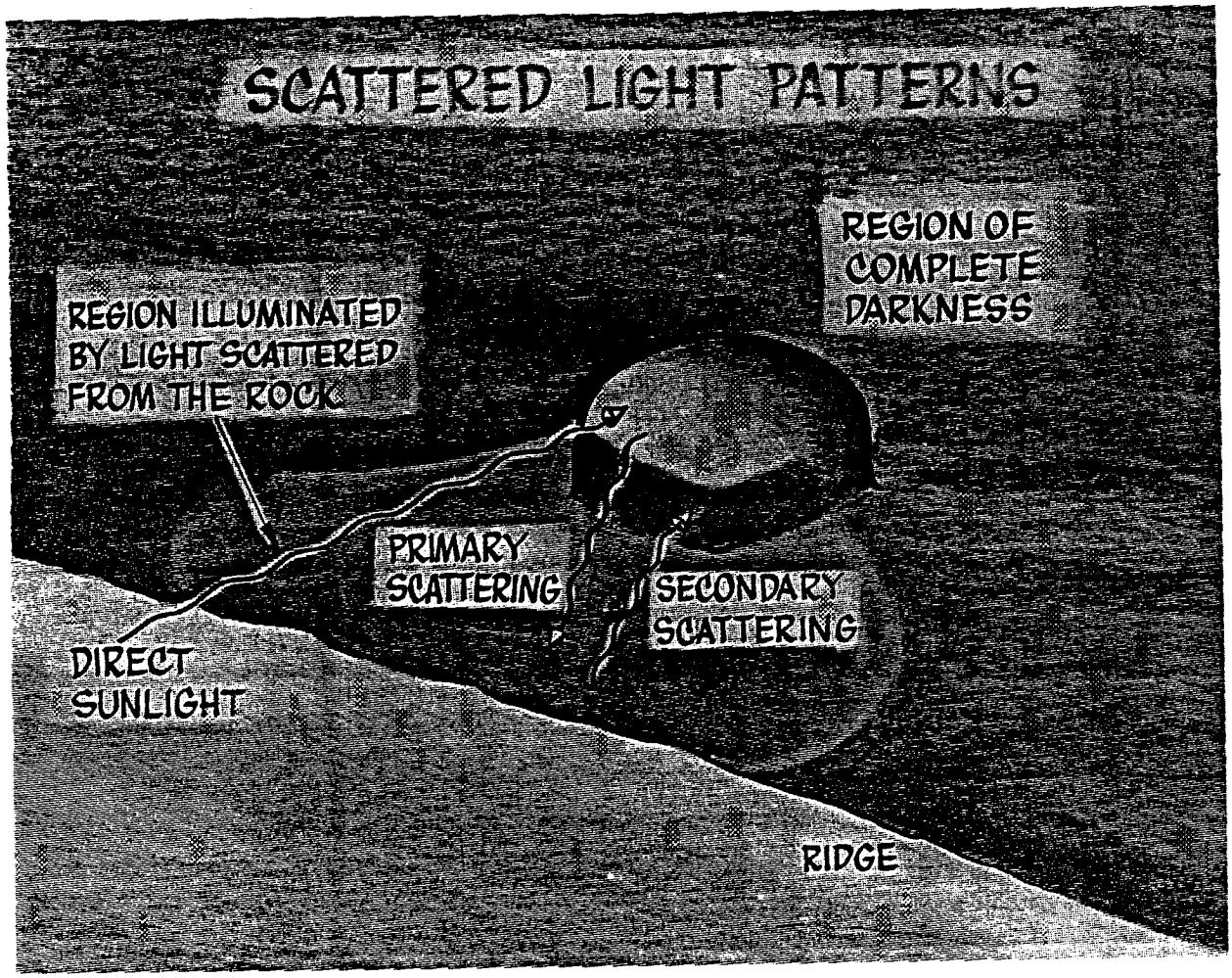

The above fig. shows the rock which is illuminated by sunlight showing the side lighted and dark side of the rock.

The illuminated size emits electrons and light due to sunlight and this is called primary scattering and the soil illuminated by rock further scatters electrons. secondary electrons.

NOZZLE CALCULATIONS

- USING PROPERTY RELATIONS FOR ISENTROPIC FLOW OF A PERFECT GAS (REF.: SAAD [47.]) (CO_2)

1. CRITICAL PROPERTIES - AT NOZZLE THROAT (EXIT); CHOKED FLOW - DENOTED BY '*'

$$T^* = \left(\frac{2}{\gamma+1}\right) T_o \qquad \text{Temperature}$$

$$P^* = \left(\frac{2}{\gamma+1}\right)^{\gamma/(\gamma-1)} P_o \qquad \text{Pressure}$$

$$\rho^* = \frac{P^*}{R T^*} \qquad \text{density}$$

$$V^* = \sqrt{\gamma R T^*} \qquad \text{Sonic velocity}$$

$T_o \equiv$ stagnation temperature

$P_o \equiv$ stagnation pressure

$R \equiv$ universal gas constant (189 J/kg K)

$\gamma \equiv$ specific heat ratio ($C_p/C_v \approx 1.3$; CO_2)

- initially, the stagnation temperature, T_o, was assumed to be 367 K

$$T^* = \left(\frac{2}{1.3+1}\right)(367K)$$

$$T^* = 319K$$

$$P^* = \left(\frac{2}{1.3+1}\right)^{\frac{1.3}{1.3-1}} P_o$$

$$P^* = 0.54 P_o$$

NOZZLE CALCULATIONS (Cont.)

1.(Cont.)

$$\rho^* = \frac{.54 P_o}{(189)(319)}$$

$$\rho^* = 9 \times 10^{-6} P_o$$

$$V^* = \sqrt{(1.3)(189)(319)}$$

$$V^* = 280 \text{ m/s}$$

2. MASS FLOW RATE RELATIONS COMBINED WITH EMPIRICALLY DETERMINED CONSTRAINT ON $P_o d^*$

a.) $\dot{m} = \rho^* A^* V^*$ mass flow rate

$A^* = \frac{\pi}{4}(d^*)^2$ nozzle exit cross sectional area; d^* = diameter of exit

$\rho^* = 9 \times 10^{-6} P_o$

$V^* = 280$

$$\dot{m} = 2.0 \times 10^{-3} P_o d^{*2} \quad \text{(a.)}$$

b.) $P_o d^* \leq 240 \text{ torr} \cdot \text{mm} \doteq 32 \text{ Pa} \cdot \text{m}$

LET:

$$P_o d^* = 32 \text{ Pa} \cdot \text{m} \quad \text{(b.)}$$

c.) Plug (b.) into (a):

$$\rightarrow \dot{m} = (2.0 \times 10^{-3})(32) d^*$$

NOZZLE CALCULATIONS (Cont.)

2 C.) (cont.)

mass flow rate in terms of nozzle exit diameter, d^*:

$$\dot{m} = (64 \times 10^{-3})\, d^* \qquad (c.)$$

d.) mass flow rate in terms of exit velocity, V^*, and thrust, F:

$$\dot{m} = \frac{F}{V^*}$$ recall, $V^* = 280$ m/s

initially thrust set at 50 N:

$$\dot{m} = \frac{50}{280}$$

$$\dot{m} = 0.18 \text{ kg/s}$$

e.) plug $\dot{m}$ into (c.) and solve for d^*:

$$d^* = \frac{0.18}{64 \times 10^{-3}}$$

→ $d^* = 2.8$ m too large!

(can find P_o : $P_o d^* = 32$

$P_o = 32/2.8$

$P_o = 11.5$ Pa)

NOZZLE CALCULATIONS (cont.)

3. THRUST REDUCED TO 0.3 N; 3 NOZZLES PRODUCING 0.1 N EACH (SEE APPENDIX FOR THRUST REDUCTION CALCULATIONS)

a.) $\Rightarrow$ REDUCTION IN MASS FLOW RATE AND, THUS, A REDUCTION IN NOZZLE EXIT DIAMETER;

$$\dot{m} = \frac{E}{V^*} = (64\times10^{-3})\, d^*$$ · from 2c.) & d.)

· recall, $V^* = 280\ m/s$

$$d^* = \frac{F}{V^*(64\times10^{-3})} = \frac{0.1}{(280)(64\times10^{-3})}$$

$\rightarrow$ $\underline{d^* = 5.6\ mm}$

b.) STAGNATION PRESSURE, P_o:

recall, $P_o d^* = 32\ Pa\cdot m$ (b.)

& let. $\underline{d^* = 6\times10^{-3}\ m}$ ←

$$P_o = \frac{32}{6\times10^{-3}}$$

$\rightarrow$ $\underline{P_o = 5300\ Pa}$

c.) MASS FLOW RATE, $\dot{m}$, per nozzle ($T_o = 367\ K$)

$$\dot{m} = \frac{0.1}{280}$$

$\rightarrow$ $\underline{\dot{m} = 0.36\times10^{-3}\ \frac{kg}{s} = .36\ g/s}$

THRUST CALCULATIONS FOR DUST REMOVAL

LET, P_A = Adhesion "Force per area" or pressure

(On the order of 68.9 to 1000 N/m^2;

68.9 $\frac{N}{m^2}$ for optical surfaces)

ASSUME, for a dust particle on a surface, [ref. 45]

that if, $F > \mu N$, the particle will be liberated.

- F: Tangential Force of Thrust
- μ: Coef. of Friction
- N: Normal Force of Thrust plus Adhesion Force

The nozzle produces a thrust (T) at an angle (θ) to the surface.

$$F \geq \mu N \quad , \quad \mu = 1 \text{ for worst case}$$

Subs.

$$T \cos\theta \geq (1)(P_A A_c + T \sin\theta) \qquad 1)$$

where A_c = area of ellipse being cleaned at any instant

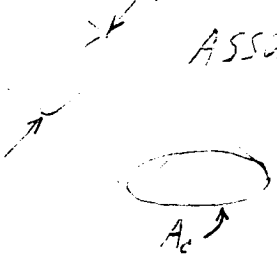

ASSUME: A) That the flow out of the nozzle is a 30° cone

B) that the flow can be considered cylindrical during impact at a diameter that varies with the "cone length"

$$A_c = \frac{\pi}{4} \frac{d_1^2}{\sin\theta} \qquad 2)$$

where d_1 is the cylindrical diameter (and minor dia of the conical ellipse) at a nozzle distance ℓ.

From 1) + 2)

$$T \cos\theta \geq P_A \frac{\pi}{4} \frac{d_1^2}{\sin\theta} + T \sin\theta \qquad 3)$$

Since T is positive
and $\sin\theta, \cos\theta$ are positive for $0 \le \theta \le 90°$

3) may be manipulated.

$$T(\cos\theta - \sin\theta) \geq P_A \frac{\pi}{4} \frac{d_1^2}{\sin\theta} \qquad 4)$$

and further

$$T(\cos\theta \sin\theta - \sin^2\theta) \geq P_A \frac{\pi}{4} d_1^2 \qquad 5)$$

One equation, 2 unknown variables θ + T, P_A + d_1 are constants for a given nozzle.

Need to maximize $(\cos\theta \sin\theta - \sin^2\theta)$ for $0° \le \theta \le 90°$
to minimize the required thrust, T.

$\theta = 22.5°$ is the optimum thrust angle

So, $\theta = \frac{\pi}{8}$ into 5) yields

$$T(.207) \geq P_A \frac{\pi}{4} d_1^2 \qquad 6)$$

or

$$T \geq 3.79 P_A d_1^2 \qquad 7)$$

THRUST CONE

d - nozzle dia.
ℓ - distance from nozzle to object
d_1 - thrust dia. at ℓ from nozzle

$$d_1 = d + 2\ell \tan 15° \qquad 8)$$

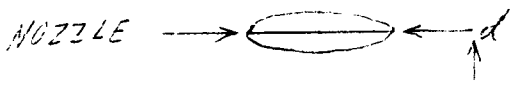

ℓ

$$A = \frac{\pi}{4} d_1^2$$

From Appendix

$$\frac{T}{280\ \frac{m}{sec}} = \left(2.5\times10^{-3}\ \frac{s}{m}\right) P \left(\frac{\pi d^2}{4}\right) \quad \text{(Nozzle Press.)} \qquad 9)$$

And the condensation constraint

$$Pd \leq 32\ \frac{N}{m} \qquad 10)$$

Combining 9) + 10) in terms of d

$$T = \left(17.59\ \frac{N}{m}\right) d \qquad 11)$$

NOZZLE DESIGN CALC's

1st ITERATION

Let, $P_A = 1000\ \frac{N}{m^2}$ (conservative)

$A = 100\ cm^2$, $d_1 = .1128\ m$

Eq. 7) gives $T \approx 50\ N$

2nd, Eq. 11) gives $d = 2.83\ m$

not reasonable.

2nd ITERATION

Let, $P_A = 270\ \frac{N}{m^2}$

$A_d = 6\ cm^2$, $\rightarrow d_1 = .0169\ m$

Eq. 7) gives $T = .3\ N$

And,

Eq. 11) $d = .017\ m$

not feasible, $\ell = 0$, nozzle touching surface

Try 3 focused nozzles,

$T = .1\ N$ each

11) $\rightarrow$ $d = 6.25\ mm$

$\ell = 2\ cm$ O.K.

NOZZLE INFORMATION

$T = .1\,N$ (each of 3)

$d = 6.25$ mm

$v = 280$ in/sec

$\dot{m} = .357$ g/sec

NOZZLE CONFIG.

Need (3) 6.25 mm dia. nozzles to focus at 2 cm, having the thrust at 2 cm fall within a 17 mm dia. circle corresponding to the thrust area diameter of $d_1 = 16.9$ mm.

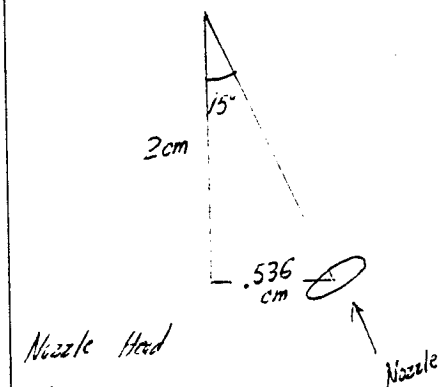

Fitting the nozzles inside a 17 mm circle and tilting each nozzle toward the center 15^{-0} accomplishes this goal.

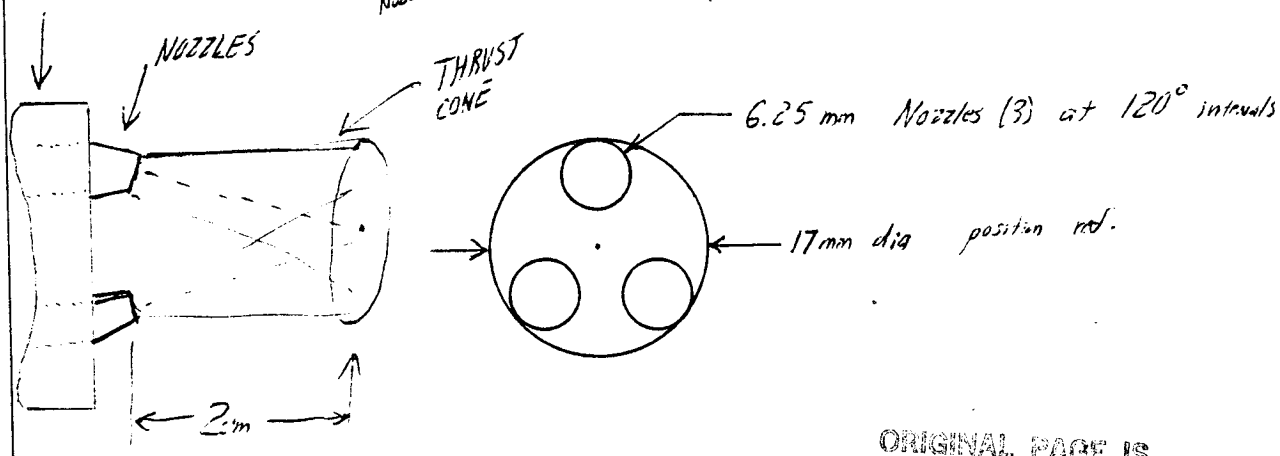

THRUST AREA

TANK VOLUME, PRESSURE, AND TEMPERATURE CALCULATIONS

1. THE TANK VOLUME WAS ARBITRARILY SET AT A 'REASONABLE' SIZE. THE TANK IS A RIGHT CIRCULAR CYLINDER WITH HEMISPHERICAL ENDS:

radius ≡ $r = 7.62\,cm$ (3 in)

height ≡ $h = 30.48\,cm$ (1.0 ft.) (w/out ends)

$$\forall_{tank} = \pi r^2 h + 4/3\,\pi r^3 \qquad \pi r^2 h + 4/3\,\pi r^3$$

$$\forall_{tank} = \pi r^2 (h + 4/3\, r)$$

$$V_{tank} = \pi (.0762\,m)^2 [(.3048\,m) + 4/3\,(.0762\,m)]$$

$$\forall_{tank} = 0.0074\ m^3$$

2. MAXIMUM TANK PRESSURE IS DEPENDENT ON THE VOLUME OF THE TANK, THE MASS OF GAS IN THE TANK, AND THE TEMPERATURE

a.) The mass of CO_2 was set according to a target operating time of 10 minutes:

$$m = \dot{m} \cdot t$$

$$\dot{m} = \underbrace{(.36\ g/s)/nozzle}_{\text{APPENDIX A: 3 c.)}} \cdot 3 \cdot (60\ s/min) \rightarrow T_o \text{ assumed to be } 367\,K$$

$$\dot{m} = 65\ g/min$$

TANK VOLUME, PRESSURE, AND TEMPERATURE CALCULATIONS (cont.)

2. a.) (cont.)

$$m = 65\ g/min\ (10\ min)$$

$$\rightarrow \underline{m = .65\ kg}$$

b.) Initially, the temperature inside the tank was assumed to be 367 K

$$T_{tank} = 367\ K$$

c.) Ideal gas law with compressibility factored in:

$$Pv = ZRT,$$

$$v = \forall / m$$

$$P\forall = m \cdot ZRT$$

$$m = \frac{P\forall}{ZRT}$$

P = pressure (Pa)

v = specific volume (m^3/kg)

Z = compressibility factor

R = universal gas constant (189 J/kg K)

T = temperature (K)

m = mass (kg)

$\forall$ = volume (m^3)

Initially, the tank is 'full' and at a maximum pressure, P_{max}. After releasing 10 minute's worth of gas, the tank is at the regulated or stagnation pressure, P_o.

TANK VOLUME, PRESSURE, AND TEMPERATURE CALCULATIONS (cont.)

2. c.) (cont.)

$$m_{initial} = \frac{P_{max} \forall_{tank}}{z_i R T_i}$$

$$m_{final} = \frac{P_o \forall_{tank}}{z_f R T_f}$$

amount of mass available for cleaning:

$$m_a = m_i - m_f$$

$m_a = 0.65\,kg$ from 2.a.)

$$\rightarrow \quad m_a = \forall_{tank}/R \left[\frac{P_{max}}{z_i T_i} - \frac{P_o}{z_f T_f} \right]$$

d.) to find P_{max}:

$$P_{max} = \left(\frac{m_a R}{\forall_{tank}} + \frac{P_o}{z_f T_f} \right) z_i T_i$$

$m_a = 0.65\,kg$

$\forall_{tank} = 0.0074\,m^3$

$R = 189\ J/kg \cdot K$

assume $T_i = T_f = 367\,K$

$P_o = 5300\,Pa$ from Appendix 3

-> need to determine z_i & z_f

TANK VOLUME, PRESSURE, AND TEMPERATURE CALCULATIONS (Cont.)

2. d.) (Cont.)

compressibility factors:

$\underline{z_f}$: $P_o = 5300$ Pa

$T_f = 367$ K

reduced pressure & temperature:

$$P_{r_o} = \frac{P_o}{P_{critical}} = 3.50 \text{ MPa}$$

$$T_{r_f} = \frac{T_f}{T_{critical}} = 304.2 \text{ K}$$

$$P_{r_o} = \frac{5300}{3.5 \times 10^6} = 1.5 \times 10^{-3}$$

$$T_{r_f} = \frac{367}{304} = 1.21$$

$\boxed{z_f = 1.0}$

Van Wylen & Sonntag [54.]

$\underline{z_i}$; since P_{max} is not known, z_i is estimated to be 0.92

$$P_{max} = \left(\frac{m_a R}{V_{tank}} + \frac{P_o}{z_f T_f} \right) z_i T_i$$

$$P_{max} = \left[\frac{(0.65)(189)}{(.0074)} + \frac{(5300)}{(1)(367)} \right] (.92)(367)$$

→ $\underline{P_{max}} = 5.6$ MPa ~ $\underline{6 \text{ MPa}}$

COMPRESSION OF CO_2 INTO TANK

When calculating the maximum Tank pressure, a temperature of 367 K was assumed. If it is assumed that the CO_2 is compressed from an initial temperature, T_1, of 300 K, & an initial pressure, P_1, of 101 kPa, the temperature will rise above the initially assumed 367 K.

1. COMPRESSION

a.) Polytropic relation for isentropic compression (assuming constant specific heats):

$$\frac{T_2}{T_1} = \left(\frac{P_2}{P_1}\right)^{k-1/k} \quad ; \quad k \equiv \gamma \equiv \text{ratio of specific heats}$$

$$T_2 = T_1\left(\frac{P_2}{P_1}\right)^{k-1/k}$$

$T_1 = 300\ K$

$P_1 = 101\ kPa$

$P_2 = 6\ MPa$

$k = 1.3$

$$T_2 = (300)\left(\frac{6\times10^6}{101\times10^3}\right)^{\frac{.3}{1.3}}$$

$$T_2 = 770\ K$$

to reduce T_2, a two stage compressor is used with perfect intercooling assumed

COMPRESSION of CO_2 INTO TANK

1. COMPRESSION (cont.)

b.) ASSUMING PERFECT INTERCOOLING & NO PRESSURE LOSSES BETWEEN STAGES, THE PRESSURE RATIO PER STAGE, r_s, IS DETERMINED FROM:

$$r_s = \sqrt[n_s]{r_t}$$

r_s = pressure ratio per stage

r_t = pressure ratio across compressor

n_s = no. of stages

$$r_t = \frac{6 \times 10^6}{101 \times 10^3}$$

$$r_t = 59$$

(REF: MARK'S STD. HANDBOOK FOR MECHANICAL ENGINEERS [5.1])

$$r_s = \sqrt[2]{59}$$

$$\rightarrow \underline{r_s = 7.7}$$

1st stage: $\rightarrow$ $T_{1a} = 300\,K$ (perfect intercooling)

$$P_{1a} = 7.7\,(101\,kPa)$$

$$P_{1a} = 778\,kPa$$

2nd stage:

$$T_2 = T_{1a}\left(\frac{P_2}{P_{1a}}\right)^{k-1/k}$$

$$T_2 = 300(7.7)^{\cdot 3/1.3}$$

$$\rightarrow \underline{T_2 = 480\,K}$$ temp. of CO_2 after compression

COMPRESSION of CO_2 INTO TANK (cont.)

2. FILLING TANK

A UNIFORM STATE, UNIFORM FLOW ANALYSIS GIVES THE FOLLOWING RELATION:

$$T_{tank} = k T_2$$

assumptions:
- adiabatic filling
- KE & PE negligable
- ideal gas

$T_{tank} = 1.3(480K)$

→ $\underline{T_{tank} = 624\ K}$

(REF: Howell & Buckius [29.7])

3. THE TEMPERATURE IN THE TANK UPON FILLING IS GREATER THAN THE TEMPERATURE ASSUMED INITIALLY, 367K, SO THE MASS OF CO_2 IN THE TANK WILL BE SMALLER THAN THAT ORIGINALLY CALCULATED.

$$M_{available} = \frac{\forall_{tank}}{R}\left[\frac{P_{max}}{Z_i T_i} - \frac{P_o}{\cancel{Z_f} T_f}\right]$$

($Z_f \approx 1$)

(from Appendix 5 : 2.c.)

because $P_{max} >> P_o$, the P_o term is negligable so:

$$M_{available} = \frac{\forall_{tank} P_{max}}{R Z_i T_i}$$

COMPRESSION OF CO_2 INTO TANK (cont)

3. (cont.) - calculating available mass, m_a, of CO_2 in tank at new temperature, $T_{tank} = 624K$

$$m_a = \frac{\forall_{tank} P_{max}}{R Z T_{tank}}$$

$\forall_{tank} = 0.0074 m^3$

$P_{max} = 6 MPa$

$R = 189 \frac{J}{kg K}$

$T_{tank} = 624 K$

need to find Z: (see Appendix B)

$$P_r = \frac{P_{max}}{P_{critical}} = \frac{6 \times 10^6}{3.5 \times 10^6}$$

$P_r = 1.7$

$$T_r = \frac{T_{tank}}{T_{critical}} = \frac{624}{304}$$

$T_r = 2.0$

$Z \doteq 0.97$

from Compressibility Chart, FIGURE A.5 of Van Wylen & Sonntag [54.]

$$m_a = \frac{(0.0074)(6 \times 10^6)}{(189)(.97)(624K)}$$

→ $m_a = 0.39$ kg

THIS 'NEW' MASS AT THE HIGHER TANK TEMP. IS LESS THAN THAT REQUIRED FOR THE TARGET OPERATING TIME OF 10 min (see APPENDIX B)

→ BUT, BECAUSE OF THE HIGHER TANK TEMPERATURE, THE STAGNATION TEMPERATURE WILL BE HIGHER & THUS THE EXIT VELOCITY FROM THE NOZZLE WILL BE HIGHER. THIS MEANS, FOR A GIVEN THRUST THE MASS FLOW RATE IS LOW

DEPENDENCE OF MASS FLOW RATE (AND THUS, OPERATING TIME) ON STAGNATION TEMPERATURE, T_o

IN APPENDIX C, A TANK TEMPERATURE, T_{tank}, OF 625 K WAS CALCULATED, GIVING AN AVAILABLE MASS, M_a, IN THE TANK OF 0.39 kg. INITIALLY, THE REQUIRED MASS WAS DETERMINED TO BE 0.65kg FOR A TARGET OPERATING TIME OF 10 minutes. FROM THIS, WITH AN ASSUMED TEMP. OF 367 K, IT WAS CALCULATED (APPENDIX B) THAT THE TANK MUST BE PRESSURIZED TO 6 MPa. IT IS THIS HIGH PRESSURE THAT 'DROVE' UP THE TANK TEMPERATURE (SEE APPENDIX C) AND, THUS, REDUCED THE AVAILABLE MASS IN THE TANK.

THE EFFECT OF THE HIGHER TANK TEMPERATURE ON MASS FLOW RATE FROM THE NOZZLES:

ASSUME $T_o = T_{tank} = 624\ K$

$$\dot{m} = \rho^*(\pi/4)d^{*2}V^*$$

$$\rho^* = .54\,P_o/RT^*$$

$$d^* = 6.0\times10^{-3}\ m$$

$$V^* = \sqrt{kRT^*}$$

$$T^* = 0.87\,T_o$$

$$P_o = 5300\ Pa$$

} SEE APPENDIX 3

$$\dot{m} = \frac{.54(5300)(\pi/4)(6\times10^{-3})^2}{(189)(0.87)\,T_o}\sqrt{(1.3)(189)(0.87)T_o}$$

$$\rightarrow \quad \dot{m} = 7.2\times10^{-3}/\sqrt{T_o} \quad \text{per nozzle}$$

DEPENDENCE OF MASS FLOW RATE (AND THUS, OPERATING TIME) ON STAGNATION TEMPERATURE, T_o

$$\dot{m} = (7.2 \times 10^{-3} / \sqrt{T_o}) \underbrace{3}_{\text{3 nozzles}}$$

operating time, t:

$$t = \frac{m_a}{\dot{m}} \quad ; \quad m_a = 0.39 \text{ kg}$$

($P_{max} = 6$ MPa, $T_{tank} = 624$ K)

$$t = \frac{0.39 \sqrt{T_o}}{(7.2 \times 10^{-3})3}$$

$$\rightarrow \quad \underline{t = 18 \sqrt{T_o} \text{ (sec)}}$$

checking a range of stagnation temperatures:

T_o (K)	t (min)	$\dot{m}$ g/min
624	7.5	52 g/min
600	7.3	53 g/min
450	6.4	61 g/min
350	5.6	72 g/min
300	5.2	75 g/min

ENERGY REQUIREMENT TO FILL TANK

assumptions:

- 2 stage positive displacement compressor with intercooler
- 60% efficiency, η_c
- constant specific heats
- Volume flow rate, $\dot{\forall}$, set at $0.001\ m^3/s$

$\Rightarrow$ time to fill tank ~ 8 sec.

Power Calculation:

Adiabatic analysis with isentropic assumption & losses lumped into the 60% efficiency factor:
(REF: MARK'S STD. HANDBOOK for MECH. ENGINEERS [5.1])

for each stage:

$$\mathcal{P} = \frac{P_1 \dot{\forall}_1 k}{(k-1)} \left[\left(\frac{P_2}{P_1} \right)^{k-1/k} - 1 \right] \frac{1}{\eta_c} \left(\frac{Z_1 + Z_2}{2 Z_1} \right)$$

Stage 1:

$P_1 = 101\ kPa$

$P_2 = 777\ kPa$ SEE APPENDIX G

$Z_1 = 1$

$Z_2 = 0.98$ ($T_1 = T_2 = 300\ K$)

438.9

$$\mathcal{P}_1 = \frac{(101 \times 10^3)(0.001)(1.3)}{(.3)} \left[(7.7)^{3/1.3} - 1 \right] \frac{1}{.60} \left(\frac{1 + .98}{2(1)} \right)$$

$\mathcal{P}_1 = 434\ W$

ENERGY REQUIREMENT TO FILL TANK (Cont.)

Stage 2:

$P_2 = 777 kPa$

$P_3 = 6.0 MPa$

$z_2 = 0.98$ $\quad (T_2 = 300K,\ T_3 = 624K)$

$z_3 = 0.97$ $\quad$ SEE APPENDIX C

$$\mathcal{P}_2 = \frac{(777\times10^3)(0.001)(1.3)}{(.3)}\left[(7.7)^{.3/1.3} - 1\right]\frac{1}{.60}\left(\frac{.98+.97}{2(.98)}\right)$$

$$\mathcal{P}_2 = 3.4\times10^3\ W$$

Total Power, $\mathcal{P}$:

$$\mathcal{P} = \mathcal{P}_1 + \mathcal{P}_2 = 434\ W + 3.4\times10^3\ W$$

$$\rightarrow \mathcal{P} = 3.8\ kW \sim 4\ kW$$

Energy Required to fill tank, E;

$$E = \mathcal{P}\cdot t = 4\ kW\,(8\ s)\left(\frac{1\ hr}{3600\ s}\right)$$

$$\rightarrow E = 0.0089\ kW\cdot hrs$$

APPENDIX 9

THIS APPENDIX CONTAINS THE STRESS ANALYSIS EQUATIONS USED IN DETERMINING THE CONFIGURATION OF THE PRESSURE VESSEL REFERRED TO IN THE DESIGN SOLUTION. THESE EQUATIONS ARE ALSO USED TO OBTAIN VALUES FOR WALL THICKNESS, VOLUME, AND WEIGHT OF THE VESSEL. THESE EQUATIONS WERE DERIVED FROM STANDARD THIN WALLED PRESSURE VESSEL THEORY.

- CONSIDER A THIN WALLED CYLINDRICAL VESSEL SUBJECTED TO INTERNAL PRESSURE P_o. TWO MAJOR STRESSES ACT ON THE VESSEL AND MAY BE DERIVED AS FOLLOWS:

- ASSUME STRESS IN RADIAL DIRECTION IS NEGLIGIBLE.

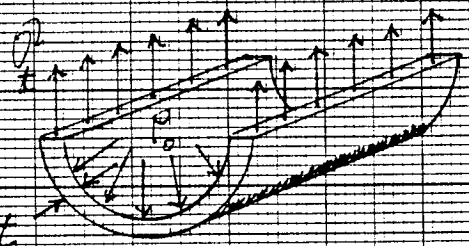

D = diameter

l = length

P_o = internal Pressure

$\Sigma F = 0$:

$$\sigma_t (2\pi l) - P_o D l = 0$$

$$\sigma_t (2\pi t l) = P_o D l$$

$$\therefore \sigma_t = \frac{P_o D l}{2\pi t l} = \frac{P_o D}{2t} \quad (1)$$

or $\sigma_t = \frac{P_o r}{t}$ for $r = \frac{D}{2}$

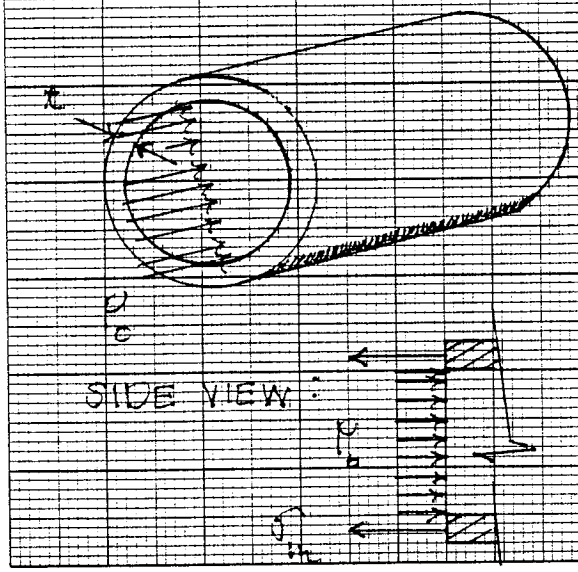

$\Sigma F = 0$:

$$-\sigma_h (\pi D t) + P_o \left(\frac{\pi D^2}{4}\right) = 0$$

$$\sigma_h (\pi d t) = P_o \left(\frac{\pi D^2}{4}\right)$$

$$\sigma_h = \frac{P_o \left(\frac{\pi D^2}{4}\right)}{\pi D t} = \frac{P_o D}{4t} \quad (2)$$

or $\sigma_h = \frac{P_o r}{2t}$

- CONSIDER A CYLINDRICAL VESSEL WITH ELLIPSOIDAL HEADS

THE EXPANSION OF THE CYLINDRICAL PORTION OF THE VESSEL IN THE RADIAL DIRECTION IS:

$$\delta_r = \frac{P_o r^2}{2tE}(2 - \mu) \qquad (3)\ [28]$$

FOR THE ELLIPSOIDAL PORTION:

$$\delta_e = \frac{P_o r^2}{tE}\left(1 - \frac{a^2}{2b^2} - \frac{\mu}{2}\right) \qquad (4)\ [28]$$

WHERE: P_o = Internal Pressure
r = radius of vessel
t = wall thickness
a = major axis of ellipse
b = minor axis of ellipse
μ = Poisson's ratio

THE DIFFERENCE IN EXPANSION PRODUCED BY THE STRESSES IN THE TWO SECTIONS OF EQUAL THICKNESS IS:

$$\delta = \delta_r - \delta_e = \frac{P_o r^2}{2tE}\left(\frac{a^2}{b^2}\right) \qquad (5)\ [28]$$

- CONSIDER A CYLINDRICAL VESSEL WITH HEMISPHERICAL HEADS

THE EXPANSION OF THE CYLINDRICAL VESSEL IS THE SAME AS BEFORE. (SEE EQUATION 3 ABOVE)
EXPANSION OF THE HEMISPHERICAL PORTION IS:

$$\delta_s = \frac{P_o r^2}{2tE}(1 - \mu) \qquad (7)\ [28]$$

THE DIFFERENCE OF THE TWO EXPANSIONS IS:

$$\delta = \delta_r - \delta_s = \frac{P_o r^2}{2tE} \qquad (8)\ [28]$$

COMPARISON OF EQUATIONS (8) AND (5) INDICATES THAT THE DEFLECTION IN THE ELLIPSOIDAL HEAD IS GREATER THAN THE CORRESPONDING DEFLECTION IN THE HEMISPHERICAL HEAD BY A FACTOR OF (a^2/b^2).

THE STRESS IN THE ELLIPSOIDAL HEAD IS ALSO GREATER THAN IN THE HEMISPHERICAL HEAD BY THE SAME AMOUNT. CONSEQUENTLY, THE MOST FAVORABLY STRESSED HEAD CONFIGURATION IS THE HEMISPHERE.

STRESS EQUATIONS MAY BE DEVELOPED FROM THE DEFLECTION FORMULA. THE EQUATIONS FOR MAXIMUM STRESS IN THE TANGENTIAL AND MERIDIONAL DIRECTIONS ARE AS FOLLOWS:

$$\sigma_m)_{max} = 0.646 \frac{P_o r}{t} \qquad (9)\ [10]$$

$$\sigma_t)_{max} = 1.032 \frac{P_o r}{t} \qquad (10)\ [10]$$

SINCE THE TANGENTIAL STRESS IN THE VESSEL IS GREATER THAN THE MERIDIONAL STRESS, EQUATION (10) WILL BE USED TO DETERMINE t.

BASED ON A FACTOR OF SAFETY, $N = 5$, AND A WELD JOINT EFFICIENCY OF 90%, AN EQUATION FOR ALLOWABLE STRESS MAY BE DERIVED.

$$\sigma_{allow} = \frac{S}{n} \eta_t \qquad (11)\ [10]$$

WHERE S IS THE STRENGTH OF THE SELECTED MATERIAL.

STRESS AND WALL THICKNESS CALCULATIONS :

- Ti - 6Al - 4V

$S_y = 135{,}000\ \#/in^2$

$n = 5 \quad \eta_t = 90\%$

$r = 3$ in.

$$P_{allow} = \frac{135{,}000\ \#/in^2}{5}\ 90\% = 24{,}300\ \#/in^2$$

$$24{,}300\ \#/in^2 = 1.032\ \frac{(841\ \#/in^2)(3'')}{t}$$

$$\therefore t = .107 \text{ in.}$$

WEIGHT CALCULATION : $\rho = 0.160\ \#/in^3 = 276.5\ \#/ft^3$

FOR CYLINDER : $\forall_{TOTAL} = \frac{\pi(.5178')^2}{4} \cdot 1' - \frac{\pi(.500')^2}{4} \cdot$

$= .0143\ ft.^3$

FOR SPHERE :

$$\forall_{TOTAL} = \frac{4}{3}\pi(.2589')^3 - \frac{4}{3}\pi(.25')^3$$

$$= .0073\ ft.^3$$

$\forall'_{TOTAL} = .0216\ ft.^3$

So $W = \rho \forall = 276.5\ \#/ft^3 \cdot .0216\ ft^3$

$W = \underline{5.96 \text{ lbs.}}$

- 17 - 7 PH Stainless Steel

$S_y = 175{,}000\ \#/in.^2$

$n = 5 \quad \eta_t = 90\% \quad r = 3$ in.

$$\sigma'_{allow} = \frac{S}{n}\eta_t = \frac{175{,}000\ \#/in^2}{5}\ 90\%$$

$$= 31{,}500\ \#/in^2$$

$$\sigma_t)_{max} = 1.032\ \frac{P_o r}{t}$$

$$t = 1.032\ \frac{P_o r}{\sigma'_{allow}}$$

$$t = \frac{1.032\,(841\ \#/in^2)(3'')}{31{,}500\ \#/in^2}$$

$$\therefore t = .083\ in.$$

WEIGHT CALCULATION : $\rho = 0.276\ \#/in^3 = 476.92\ \#/ft^3$

FOR CYLINDER :

$$\forall_{TOTAL} = \frac{\pi(.5138')^2}{4}\cdot 1' - \frac{\pi(.500')^2}{4}\cdot 1'$$

$$= .011\ ft^3.$$

FOR SPHERE :

$$\forall_{TOTAL} = \frac{4}{3}\pi(.2569')^3 - \frac{4}{3}\pi(.25')^3$$

$$= .0056\ ft^3$$

So $\forall'_{TOTAL} = 0.0166\ ft^3$

$$W = \rho\forall = 476.92\ \#/ft^3 \cdot 0.0166\ ft^3$$

$$\underline{\underline{W = 7.90\ lbs.}}$$